Available online at www.sciencedirect.com
ScienceDirect
Journal of the Mechanics and Physics of Solids
55 (2007) 2206–2236

JOURNAL OF THE MECHANICS AND PHYSICS OF SOLIDS

www.elsevier.com/locate/jmps

Objective molecular dynamics

Traian Dumitrică[a,*], Richard D. James[b]

[a]Department of Mechanical Engineering, University of Minnesota, USA
[b]Department of Aerospace Engineering and Mechanics, University of Minnesota, USA

Received 11 October 2006; received in revised form 6 January 2007; accepted 3 March 2007

Abstract

We introduce a generalization of periodic molecular dynamics that we term *objective molecular dynamics*. It is a method of doing molecular dynamics for a restricted set of atoms, nonperiodically mapping the time-dependent displacements of this small set of atoms onto the full, typically infinite structure, such that the full structure satisfies exactly the full, unconstrained set of equations of molecular dynamics subject to certain group-invariant initial conditions. The method is applicable to a wide variety of interesting molecular structures including the tails, capsids and other parts of many viruses, carbon nanotubes, many of the common proteins, C_{60} and many other nanostructures now being synthesized, especially via the process of self-assembly. The method is illustrated by simulations of carbon nanotubes.

Keywords: Atomistic structures; Numerical algorithms; Buckling; Structures; Dynamics

1. Introduction

The most common way to implement molecular dynamics is via periodic molecular dynamics (Allen and Tildesley, 1987; Parrinello and Rahman, 1980; Toukan et al., 1983; Rurali and Hernandez, 2003) and this is the version that is often found as subroutines of quantum mechanics codes. In this method one can assign the periodicity completely independently of the type of atom or force law. The method can be adapted to isolated systems by simply assigning the period to be much larger than the typical lattice parameter

*Corresponding author.
E-mail addresses: td@me.umn.edu (T. Dumitrică), james@umn.edu (R.D. James).

0022-5096/$ - see front matter © 2007 Elsevier Ltd. All rights reserved.
doi:10.1016/j.jmps.2007.03.001

of the substance and assigning the initial data appropriately, so that the collection of atoms does not substantially interact with its periodic images for $t>0$.

In periodic molecular dynamics atom i with mass m_i and position $\mathbf{x}_i(t)$ in the unit cell is subject to the equations of motion

$$m_i\ddot{\mathbf{x}}_i = -\frac{\partial\varphi}{\partial\mathbf{x}_i} \quad \text{no sum over } i, \tag{1}$$

where the right-hand side accounts for the forces, in principle, exerted on i by the full set of atoms in the periodic structure, or at least the atoms that fall within the cutoff, if there is one. However, the positions of atoms in all other cells are not found by solving (1). Rather they are forced to adopt the positions given by the assigned periodicity: atoms with mass m_i are forced to adopt positions $\mathbf{x}_i(t)+v^i\mathbf{e}_i$ where the v^1, v^2, v^3 are integers and the linearly independent vectors $\mathbf{e}_1, \mathbf{e}_2, \mathbf{e}_3$ define the periodicity. At first sight, it might seem like there is an inherent contradiction in the method—that the atoms in the other unit cells are forced to go to certain places rather than to the places they would go if freely allowed to satisfy the equations of motion—but, as is well known, there is no such contradiction. That is, under physically natural hypotheses on the potential energy surface φ, the full set of equations of molecular dynamics for all the atoms has an invariant manifold associated with arbitrarily assigned periodicity. That is, if the initial data are periodic in an appropriate sense, the unconstrained unique solution of the equations of motion of all the atoms retains exactly this periodicity. Besides mild conditions of smoothness of φ, the key hypotheses on φ that are needed to prove this theorem are (1) translation invariance, $\varphi(\mathbf{x}_1+\mathbf{c}, \mathbf{x}_2+\mathbf{c}, \ldots)=\varphi(\mathbf{x}_1, \mathbf{x}_2, \ldots)$ for all $\mathbf{x}_1, \mathbf{x}_2, \ldots$ and for all $\mathbf{c}$, and (2) invariance under permutations of atoms of like species: $\varphi(\mathbf{x}_{\Pi(1)}, \mathbf{x}_{\Pi(2)}, \ldots)=\varphi(\mathbf{x}_1, \mathbf{x}_2, \ldots)$, where Π is a permutation of $\{1, 2, \ldots\}$ that preserves species, i.e., atomic mass and number. Translation invariance and permutation invariance are properties of, say, a ground state potential energy φ that comes from general quantum mechanics under the Born–Oppenheimer approximation, in which case the $\mathbf{x}_1, \mathbf{x}_2, \ldots$ are the ionic positions.

The method gives substantial simplification, because the equations of motion only have to be solved for the atoms in the unit cell, and, if there is a cutoff, forces also only need to be evaluated for a finite set of atoms. It is widely believed that if the unit cell is chosen to contain a sufficient but modest number of atoms, and the periodicity is set properly, periodic molecular dynamics gives many statistical properties that would be exhibited by crystals composed of the atoms used in the simulation. Also, if one varies the periodicity, then one can vary systematically the macroscopic stress in the crystal.

In this paper we introduce a simple but broad generalization of periodic molecular dynamics that we term *objective molecular dynamics*. Its existence and potential usefulness follow from two simple observations. First, the potential energy that comes from full quantum mechanics under the Born–Oppenheimer approximation, as described above, is actually fully frame-indifferent, in the sense that $\varphi(\mathbf{Q}\mathbf{x}_1+\mathbf{c}, \mathbf{Q}\mathbf{x}_2+\mathbf{c}, \ldots)=\varphi(\mathbf{x}_1, \mathbf{x}_2, \ldots)$ for all $\mathbf{x}_1, \mathbf{x}_2, \ldots$ and for all $\mathbf{c}$ and for all $\mathbf{Q}\in \mathrm{O}(3)$, where O(3) denotes the full orthogonal group in three dimensions (Section 3.2). This fact, combined with the permutation invariance described above, implies a much bigger invariant manifold than the one that is exploited in periodic molecular dynamics. Second, the molecular structures that are associated to this invariance contain some of the most widely studied structures in science: carbon nanotubes, C_{60}, viral capsids and many viral parts (necks, tails, baseplates), many of the common proteins (actin, GroEL, hemoglobin, potassium channel, collagen),

bilayers (staggered and unstaggered), and various kinds of molecular fibers; see James (2006) for many examples. For reasons discussed in Caspar and Klug (1962), Crane (1950) and James (2006), structures that are made by the process of self-assembly naturally give rise to objective structures. Some of these structures have no 3, 2 or 1-D periodicity, and therefore periodic molecular dynamics would not be applicable. Furthermore, even in the case of a fiber or helical structure with 1-D periodicity, objective molecular dynamics allows one to apply and vary forces and moments in ways that are not possible in periodic molecular dynamics.

In objective molecular dynamics one gives a fundamental domain, a group, and initial conditions for a set of atoms on the fundamental domain. The motions of atoms of the whole structure are then determined by the group acting on the atoms in the fundamental domain. Forces on atoms in the fundamental domain are computed from all other atoms of the structure. Thus, an analogous simplification as is found in periodic molecular dynamics occurs in objective molecular dynamics. If, in objective molecular dynamics, the group chosen is translations $v^i\mathbf{e}_i$ as defined above, then objective molecular dynamics reduces to periodic molecular dynamics. Objective molecular dynamics can simulate certain kinds of large scale transient dynamic modes, in addition to the statistically stationary ones; the nature of these modes is determined by the group.

This method of molecular dynamics would seem to be particularly useful for the study of phase transformation and defect motion in nanostructures. In fact, the formulas for objective molecular structures were abstracted from a study of the phase transformation in bacteriophage T4 tail sheath (Falk and James, 2006). Pictures of the two phases in this case are shown in the bottom left of Fig. 1. In addition, defects like the Stone–Wales defect

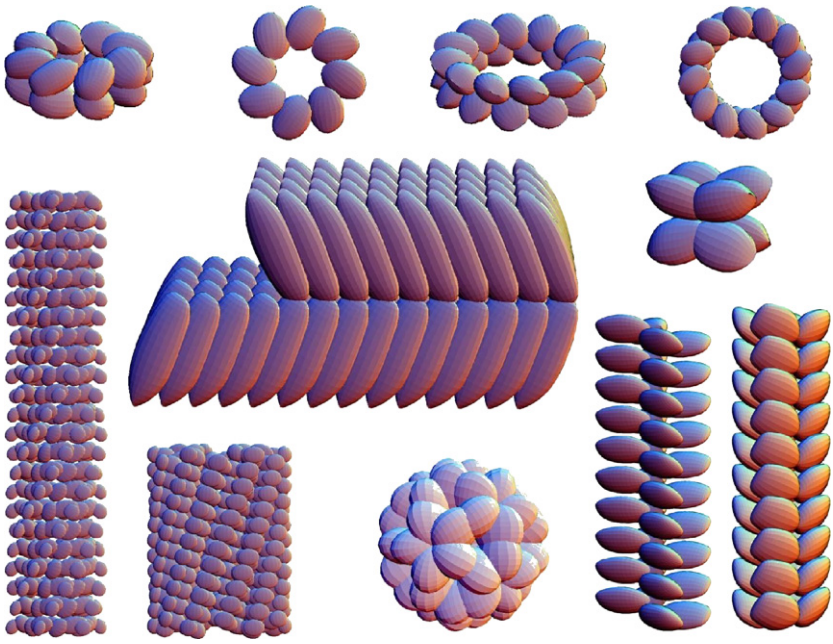

Fig. 1. Some objective molecular structures. These are all given by the formulas (4)–(7) with various choices of the parameters. In each case the molecule is represented by a kind of unsymmetric blob.

(Dumitrică et al., 2006) that can propagate in a helical fashion in a carbon nanotube would seem good candidates for objective molecular dynamics.

The plan of this paper is as follows. In Section 2 we summarize some results of James (2006) on *objective structures*. These are the structures to which objective molecular dynamics applies, or, more precisely, the symmetry groups of these structures are the basis of objective molecular dynamics. In Section 2 some formulas are given that always produce such structures, and the symmetry groups are extracted from these formulas. In Section 3.1 the basic abstract theorem underlying objective molecular dynamics is given, followed in Sections 3.3–3.5 by concrete cases that relate specifically to the formulas given in Section 2. In Section 4 we consider an illustrative example: the dynamics of carbon nanotubes. In Sections 4.1–4.2 we discuss carbon nanotubes as objective molecular structures and make the connection with the widely used (n,m) hexagonal-lattice notation. The actual implementation of the abstract ideas requires the development of some technology concerning the delineation of the group and corresponding fundamental domain which we develop in Section 4.3.

In Section 4.4.1 we outline the modifications needed to transform classical molecular dynamics into objective dynamics. Section 4.4.2 presents performed objective molecular dynamics simulations on various carbon nanotubes. Unlike periodic molecular dynamics, general objective molecular dynamics can exhibit transient dynamic modes on a scale that is much larger than the size of the fundamental domain. We show how the energy of one of these large-scale transient breathing modes becomes distributed into atomic scale vibrations. Next we discuss the statics and dynamics of carbon nanotubes under applied twist. This is a useful illustration of the method because we can *continuously* apply twist, which cannot be done in periodic molecular dynamics. We first verify that the accepted linearized properties of a carbon nanotube can be obtained with a small fundamental domain. Then we consider a nanotube under applied twist and constant length. We are able to nicely define a dramatic torsional instability that occurs near a value of twist of $2^\circ/\text{nm}$, see Fig. 9 and Section 4.4.2. Finally, we indicate how objective method can be used to study bending deformations in nanotubes.

An objective molecular structure has *structural parameters*, i.e., parameters that can be varied while retaining its property of being an objective structure, these being analogous to the lattice vectors $\mathbf{e}_1, \mathbf{e}_2, \mathbf{e}_3$ in periodic molecular dynamics. In the latter these are conjugate to applied stresses, and the expectation is similar in objective molecular dynamics. But in objective molecular dynamics the nature of these "applied stresses" may vary widely with the group; for a group appropriate to a carbon nanotube these are evidently the applied axial force and axial moment. It is a fascinating question of what they might be in general, but we postpone that to forthcoming work. Even in the periodic case, the issue of what is the "stress" corresponding to a molecular dynamics simulation is somewhat controversial, as indicated by the divergent definitions of stress found in the literature (Costanzo et al., 2005; Hardy, 1982; Murdoch and Bedeaux, 1994; Zhou, 2005; Zimmerman et al., 2004). Results along these lines for objective molecular dynamics are important because they are needed to be able to plot, for example, a torque–twist relation for a carbon nanotube based on fully dynamic simulations.

We conclude this introduction with three observations. First, it appears in our simulations that objective molecular dynamics may be a "natural" method for objective structures, in the sense that low energy modes that would contribute strongly to properties calculated via statistical mechanics would be captured using small fundamental domains.

The precise meaning of this awaits further study. Second, since objectivity, i.e., full frame-indifference, extends to more general situations than full quantum mechanics under the Born–Oppenheimer approximation—some situations for example in which the nuclear positions are quantized or the electrons are treated dynamically—then it appears that objective molecular dynamics has possible generalizations in these directions. However, in the relativistic case, Lorentz invariance would give rise to other (interesting) issues. Third, we note that objective molecular dynamics would seem to be especially useful in the context of large scale simulations of viruses (see, e.g., Freddolino et al., 2006), giving substantial speedup. For reasons most likely arising from the special relation between objective structures and the process of self-assembly, viruses contain many objective structures, e.g., capsids, necks, tails and baseplates, as well as specialized structures for packing DNA, all tend to be objective molecular structures.

Notation. The summation convention is used here. $\mathbb{Z}$ is the integers and $\mathbb{Z}^3$ is the set of triples of integers. Unless indicated otherwise, Greek letters are scalars, lower case Latin letters are vectors in $\mathbb{R}^3$. Typically, uppercase Latin letters represent 3×3 matrices, except in Section 3.1 where they denote either infinite collections of vectors or else group operations and in Section 4.4 where they denote quantities associated with the subgroup used to define the MD simulations we do for the carbon nanotube. $\mathbf{A}^i$ denotes $\mathbf{A}$ multiplied by itself i times, if i is a positive integer, or $\mathbf{A}^{-1}$ multiplied by itself $|i|$ times if i is a negative integer. The letters $\mathbf{Q}$ and $\mathbf{R}$, variously decorated, are reserved for matrices in $\mathrm{O}(3)=\{\mathbf{R}:\mathbf{R}^{\mathrm{T}}\mathbf{R}=\mathbf{I}\}$; here, the superscript T indicates the transpose, and $\mathbf{I}$ is the 3×3 identity matrix. The upper limit of all summations in this paper can take positive or negative integer values. If the upper limit is nonnegative, the summation has its usual meaning; for negative values the meaning is

$$\sum_{i=0}^{r} a_i=\begin{cases}0, & r=-1,\\ -a_{-1}-a_{-2}-\cdots-a_{r+1}, & r<-1.\end{cases} \tag{2}$$

Finally, we note that subscripts of vectors and matrices in this paper do not signify components; instead, they label molecules and atoms within molecules.

2. Objective structures and their symmetry groups

Informally, an objective molecular structure is a finite or infinite collection of identical molecules, each of which is composed of M atoms, such that corresponding atoms in different molecules see exactly the same environment up to orthogonal transformation. More precisely, a collection of position vectors $\mathscr{S}=\{\mathbf{x}_{i,j}: i=1,\dots,N,\ j=1,\dots,M\}$ is an *objective molecular structure* if there exists NM orthogonal matrices $\{\mathbf{R}_{1,1},\dots,\mathbf{R}_{N,M}\}$ such that

$$\mathscr{S}=\{\mathbf{x}_{i,k}+\mathbf{R}_{i,k}(\mathbf{x}_{n,m}-\mathbf{x}_{1,k}): n=1,\dots,N,\ m=1,\dots,M\}\quad(\text{no sum over } k) \tag{3}$$

for every choice of $i\in\{1,\dots,N\}, k\in\{1,\dots,M\}$. The connection with other related work is discussed in James (2006). The terminology "objective" relates to the connection between these structures and the fundamental invariance group of quantum mechanics, see Section 3.2 below.

The main points about this definition are the following. First, in the notation $\mathbf{x}_{i,j}$, i denotes the molecule while j denotes the atom within the molecule: one can say that $\mathbf{x}_{i,j}$ is

the position of atom j within molecule i. N can be infinite but M is always finite. In words, the definition says that one can consider the entire structure from the point of view of atom k of molecule 1, $(\mathbf{x}_{n,m} - \mathbf{x}_{1,k})$, do a suitable orthogonal transformation, $\mathbf{R}_{i,k}$, add the result to atom k of molecule i, $(\mathbf{x}_{i,k})$, and restore the entire structure. The key point is that the left-hand side of (3) is independent of i and k ("same structure"), and the definition holds for all i, k. Note that it is important that the second index labeled k appears three times, in the indicated places, in this definition. If there is only one atom per molecule ($M = 1$) we say the structure is an *objective atomic structure*.

While the definition of an objective molecular structure refers only to the local environment of corresponding atoms in different molecules, there is a close relation to symmetry groups, in particular, groups of isometries (i.e., groups of transformations of the form $\mathbf{Qx} + \mathbf{c}, \mathbf{Q} \in \mathrm{O}(3), \mathbf{c} \in \mathbb{R}^3$) in 3-D. This is discussed in James (2006), Section 6.1. For the calculations done here, we have found the formulas like those given below to be easier to use than the generators of those groups. In particular, for the example of the twisting of a nanotube discussed below, the groups would change drastically with the angle of twist, while the parameters in these formulas can be varied continuously. Objective molecular dynamics can be phrased entirely in terms of these parameters.

For physical applications we adopt two additional assumptions on objective structures. We say that the structure *preserves species* if the atomic mass and number of atom (i, k) is the same as that of (j, k) for all $i, j = 1, \ldots, N$ and all $k = 1, \ldots, M$. An objective structure is *discrete* if there exists a fixed $r > 0$ such that the collection of balls of radius r centered on every atom is a pairwise disjoint collection.

We sometimes use different ways of indexing the molecule that are adapted to some formulas for objective structures given below. That is, we replace i in $\mathbf{x}_{i,k}$ by a set of two integers (p, q), by writing $\mathbf{x}_{(p,q),k}$, or three integers (p, q, r), writing $\mathbf{x}_{(p,q,r),k}$, and use, respectively, the indexing sets $\mathbb{Z}^2$ or $\mathbb{Z}^3$ for the molecules. We note that a structure can be an objective molecular structure, but the "molecule" not be the actual physical molecule as usually understood. This does not invalidate the theory. In fact, for many objective molecular structures the molecule as embodied in (3) is the actual physical molecule.

In James (2006) several explicit formulas are given for objective molecular structures. These formulas give objective molecular structures independent of the structure of the molecule. The molecule is denoted by assigned position vectors $\mathbf{p}_1, \ldots, \mathbf{p}_M$.

1. Finite structures. In this case N is finite and a finite subgroup of O(3), $\mathbf{Q}_1, \ldots, \mathbf{Q}_N$, is given with $\mathbf{Q}_1 = \mathbf{I}$, and $\mathbf{y}_1$ is a given vector in $\mathbb{R}^3$.

$$\mathbf{x}_{i,j} = \mathbf{Q}_i(\mathbf{y}_1 + \mathbf{p}_j), \quad i = 1, \ldots, N, \ j = 1, \ldots, M. \tag{4}$$

2. Two-term formula

$$\mathbf{x}_{(p,q),k} = \mathbf{x}_1 + \sum_{i=0}^{p-1} \mathbf{R}_2^i \mathbf{t}_2 + \mathbf{R}_2^p \sum_{i=0}^{q-1} \mathbf{R}_1^i \mathbf{t}_1 + \mathbf{R}_2^p \mathbf{R}_1^q \mathbf{p}_k, \quad k = 1, \ldots, M, \tag{5}$$

where p, q are integers, $\mathbf{R}_1, \mathbf{R}_2 \in \mathrm{O}(3)$ and $\mathbf{t}_1, \mathbf{t}_2 \in \mathbb{R}^3$, satisfy the restrictions

$$(\mathbf{R}_2 - \mathbf{I})\mathbf{t}_1 = (\mathbf{R}_1 - \mathbf{I})\mathbf{t}_2, \quad \mathbf{R}_1\mathbf{R}_2 = \mathbf{R}_2\mathbf{R}_1. \tag{6}$$

3. Three-term formula

$$\mathbf{x}_{(p,q,r),k} = \sum_{i=0}^{p-1} \mathbf{R}_3^i \mathbf{t}_3 + \mathbf{R}_3^p \sum_{j=0}^{q-1} \mathbf{R}_2^j \mathbf{t}_2 + \mathbf{R}_3^p \mathbf{R}_2^q \sum_{k=0}^{r-1} \mathbf{R}_1^k \mathbf{t}_1 + \mathbf{x}_1 + \mathbf{R}_3^p \mathbf{R}_2^q \mathbf{R}_1^r \mathbf{p}_k, \tag{7}$$

where $\mathbf{R}_1, \mathbf{R}_2, \mathbf{R}_3 \in \mathrm{O}(3)$ and $\mathbf{t}_1, \mathbf{t}_2, \mathbf{t}_3 \in \mathbb{R}^3$ satisfy the restrictions

$$\begin{aligned} &\mathbf{t}_3 + \mathbf{R}_3\mathbf{t}_2 = \mathbf{t}_2 + \mathbf{R}_2\mathbf{t}_3, \quad \mathbf{R}_3\mathbf{R}_2 = \mathbf{R}_2\mathbf{R}_3, \\ &\mathbf{t}_3 + \mathbf{R}_3\mathbf{t}_1 = \mathbf{t}_1 + \mathbf{R}_1\mathbf{t}_3, \quad \mathbf{R}_3\mathbf{R}_1 = \mathbf{R}_1\mathbf{R}_3, \\ &\mathbf{t}_2 + \mathbf{R}_2\mathbf{t}_1 = \mathbf{t}_1 + \mathbf{R}_1\mathbf{t}_2, \quad \mathbf{R}_2\mathbf{R}_1 = \mathbf{R}_1\mathbf{R}_2. \end{aligned} \tag{8}$$

The two-term formula is a special case of the three-term formula (put $\mathbf{t}_1 = 0, \mathbf{R}_1 = \mathbf{I}$ in (7), (8)). We include both because a single-walled carbon nanotube, which we discuss in detail later, is given by the two-term formula, and also because, if one compares the two- and three-term formulas, one can immediately guess by analogy an n-term formula, with associated restrictions, and this also gives objective molecular structures.

These formulas give lots of these structures. The three-term formula gives an arbitrary ordered periodic crystal lattice, by the choice $\mathbf{R}_1 = \mathbf{R}_2 = \mathbf{R}_3 = \mathbf{I}$. Some other typical structures produced by these three formulas are shown in Fig. 1, illustrated with a choice of $\mathbf{p}_1, \ldots, \mathbf{p}_M$ that produces an unsymmetrical blob-like molecule, so that the relationships between molecules can be seen.

We should point out that the ℓ-term formula ($\ell \geqslant 1$) sometimes gives a finite structure, even though the indexing set is infinite. In such cases, for large values of the first index, the molecules fall precisely on molecules previously constructed; these become discrete objective molecular structures by restricting in a suitable way the indices $(p, q, r, \ldots)$. Also, for some choices of the $\mathbf{t}$'s and $\mathbf{R}$'s the structures are infinite but not discrete (though, as stated above, they are always objective molecular structures). We deal with this explicitly in our application to the carbon nanotube.

Now we extract some subgroups of the symmetry groups of structures given by these formulas that will be useful for objective molecular dynamics. Of interest here are isometry groups of the structure $\mathscr{S}$, i.e., groups of orthogonal transformations and translations $(\mathbf{Q}|\mathbf{c})$ that satisfy

$$\mathbf{Q}\mathscr{S} + \mathbf{c} = \mathscr{S}. \tag{9}$$

These transformations form a group under the usual operations $(\mathbf{Q}_2|\mathbf{c}_2) \circ (\mathbf{Q}_1|\mathbf{c}_1) = (\mathbf{Q}_2\mathbf{Q}_1|\mathbf{Q}_2\mathbf{c}_1 + \mathbf{c}_2)$. We just record the case of the finite groups and those of the three-term formula; the corresponding group for the n-term form is then easily found by analogy. The results are given below in the same notation as the preceding enumeration.

1. Finite structures. These are obvious: $(\mathbf{Q}|\mathbf{c}) = (\mathbf{Q}_i|0),\ i = 1, \ldots, N$.
2. Three-term formula. In this case $(\mathbf{Q}|\mathbf{c})$ are given by

$$\mathbf{Q} = \mathbf{Q}_{p,q,r} = \mathbf{R}_3^p \mathbf{R}_2^q \mathbf{R}_1^r, \quad \mathbf{c} = \mathbf{c}_{p,q,r} = \sum_{i=0}^{p-1} \mathbf{R}_3^i \mathbf{t}_3 + \mathbf{R}_3^p \sum_{j=0}^{q-1} \mathbf{R}_2^j \mathbf{t}_2 + \mathbf{R}_3^p \mathbf{R}_2^q \sum_{k=0}^{r-1} \mathbf{R}_1^k \mathbf{t}_1 - \mathbf{R}_3^p \mathbf{R}_2^q \mathbf{R}_1^r \mathbf{x}_1. \tag{10}$$

That these are symmetry groups of the given structures is proved by direct (but messy) calculations (see James, 2006). We note also a related interesting fact: if one rearranges (9) and (10), one gets

$$\mathbf{x}_{(p,q,r),k} + \mathbf{Q}_{p,q,r}(\mathbf{x}_{(j,k,l),\ell} - \mathbf{x}_{(0,0,0),k}) = \mathbf{x}_{(p+j,q+k,r+l),\ell}. \tag{11}$$

This shows immediately that the structure given by the three-term formula describes an objective molecular structure, with molecule "1" in the basic definition (3) being labelled by $(0,0,0)$. Note that in this case $\mathbf{Q}_{p,q,r}$ does not depend on the molecule. The reasons for this, and a deeper discussion of the relation between group and structure, are given in James (2006).

3. Objective molecular dynamics

3.1. Abstract form of the argument

We write the equations of molecular dynamics in a schematic way. $\mathbf{X}$ is shorthand for $\mathbf{x}_{i,j}, i = 1,\ldots,N,\ j = 1,\ldots,M$, and we let $n = NM$; typically $N = \infty$.

We are interested in time-dependent mappings $\mathbf{X} : [0, T) \to \mathbb{R}^n$ satisfying the initial value problem:

$$\begin{aligned} \mathbf{M}\ddot{\mathbf{X}} &= -\nabla\Phi(\mathbf{X}),\\ \mathbf{X}(0) &= \mathbf{X}_0,\\ \dot{\mathbf{X}}(0) &= \mathbf{V}_0, \end{aligned} \tag{12}$$

with $\mathbf{X}_0, \mathbf{V}_0 \in \mathbb{R}^n$ n-dimensional vectors, the mass matrix $\mathbf{M} : \mathbb{R}^n \to \mathbb{R}^n$ is a linear transformation on $\mathbb{R}^n$ and $\nabla\Phi : \mathbb{R}^n \to \mathbb{R}^n$. We assume conditions on $\nabla\Phi$ such that this system has a unique solution for all choices of $(\mathbf{X}_0, \mathbf{V}_0) \in \mathscr{I}$. Here, $\mathscr{I}$ will be a suitably chosen set that, for example, avoids singularities associated with two ions occupying the same position. There is assumed to be a group $\mathscr{G}$ of affine transformations that act on $\mathbb{R}^\infty$ of the form

$$\mathbf{X} \to \mathbf{T}\mathbf{X} = \mathbf{T}'\mathbf{X} + \mathbf{C}. \tag{13}$$

The group operation is composition: $\mathbf{G}_1(\mathbf{G}_2\mathbf{X}) = \mathbf{T}'_1\mathbf{T}'_2\mathbf{X} + \mathbf{T}'_1\mathbf{C}_2 + \mathbf{C}_1$. There is also a subgroup $\mathscr{G}'$ obtained by putting $\mathbf{C} = 0$. The mass matrix is assumed to be invariant in the sense that $\mathbf{M} = \mathbf{T}'\mathbf{M}(\mathbf{T}')^{-1}$ for all $\mathbf{T}' \in \mathscr{G}'$. The potential Φ is assumed to be equivariant in the sense that

$$\nabla\Phi(\mathbf{T}\mathbf{X}) = \mathbf{T}'\nabla\Phi(\mathbf{X}) \tag{14}$$

holds for all $\mathbf{X}$, and the set of initial conditions is also assumed to be invariant: if $(\mathbf{X}_0, \mathbf{V}_0) \in \mathscr{I}$, then $(\mathbf{T}\mathbf{X}_0, \mathbf{T}'\mathbf{V}_0) \in \mathscr{I}$ for all $\mathbf{G} \in \mathscr{G}$, with $\mathbf{T}, \mathbf{T}'$ related by (13).

Consider initial data that are group invariant in the sense that

$$\begin{aligned} \mathbf{T}\mathbf{X}_0 &= \mathbf{X}_0,\\ \mathbf{T}'\mathbf{V}_0 &= \mathbf{V}_0, \end{aligned} \tag{15}$$

for all $\mathbf{T} \in \mathscr{G}$. Then the solution corresponding to this initial data is invariant, in the sense that

$$\mathbf{T}\mathbf{X}(t) = \mathbf{X}(t), \quad t \in [0, T) \tag{16}$$

for all $\mathbf{T} \in \mathcal{G}$. The proof is trivial. Consider the solution $\mathbf{X}(t)$ and define for a fixed $\mathbf{T} \in \mathcal{G}$

$$\mathbf{Y}(t) = \mathbf{T}^{-1}\mathbf{X}(t) = (\mathbf{T}')^{-1}(\mathbf{X}(t) - \mathbf{C}). \tag{17}$$

Then, substituting $\mathbf{X}(t) = \mathbf{T}\mathbf{Y}(t) = \mathbf{T}'\mathbf{Y}(t) + \mathbf{C}$ into (12), we get

$$\mathbf{M}\mathbf{T}'\ddot{\mathbf{Y}} = -\nabla\Phi(\mathbf{T}\mathbf{Y}). \tag{18}$$

Using the invariances of $\mathbf{M}$, Φ and of the initial data, we get:

$$\begin{aligned} \mathbf{M}\ddot{\mathbf{Y}} &= -\nabla\Phi(\mathbf{Y}), \\ \mathbf{Y}(0) &= \mathbf{X}_0, \\ \dot{\mathbf{Y}}(0) &= \mathbf{V}_0. \end{aligned} \tag{19}$$

Thus, $\mathbf{Y}(t)$ satisfies the same initial value problem as $\mathbf{X}(t)$ and, therefore, by uniqueness, $\mathbf{Y}(t) = \mathbf{X}(t)$, $0 \leqslant t < T$. Since $\mathbf{T} \in \mathcal{G}$ was arbitrary, then, accounting for the relation between $\mathbf{X}(t)$ and $\mathbf{Y}(t)$, we have

$$\mathbf{X}(t) = \mathbf{T}\mathbf{X}(t) \tag{20}$$

for all $\mathbf{T} \in \mathcal{G}$.

The actual group action, in components, corresponding to the various formulas given in Section 2, is given explicitly below in Sections 3.3–3.5.

3.2. Invariance of the potential energy

We now discuss the invariance of the potential energy, or, more precisely, of the forces. We use a fairly general format of defining the potential energy of the atomic system from the ground state energy of full quantum mechanics under the Born–Oppenheimer approximation. Various simpler models, such as density functional theory or semi-empirical force fields, inherit this invariance.

We use the basic notation of objective molecular structures even though the atoms in this section are *not* assumed to belong to such a structure.[1] Thus we assume nuclear positions $\mathbf{x}_{i,j}, i = 1, \ldots, N,\ j = 1, \ldots, M$ with M finite and N finite or infinite. We also assume that nuclei (i,j) with a fixed value of the second index j all have the same atomic number $Z^{(j)}$. The ground state energy is obtained by minimizing the sum of terms representing the kinetic energy (KE), the electron–electron interaction energy (EE), the electron–nuclear energy (EN) and the nuclear–nuclear energy (NN) over antisymmetric normalized wave functions:

$$\begin{aligned} &\varphi(\mathbf{x}_{1,1}, \ldots, \mathbf{x}_{1,M} \ldots, \mathbf{x}_{N,1}, \ldots, \mathbf{x}_{N,M}) \\ &\quad = \min(\mathrm{KE} + \mathrm{EE} + \mathrm{EN} + \mathrm{NN}) \\ &\quad = \min_{\substack{\psi \text{ anti-symmetric} \\ \text{normalized}}} \sum_{\substack{s_1,\ldots,s_P \\ = \pm\frac{1}{2}}} \left(\int_{\mathbb{R}^{3P}} \frac{1}{2} |\nabla\psi((\mathbf{r}_1, s_1), \ldots, (\mathbf{r}_P, s_P))|^2 \, \mathrm{d}\mathbf{r}_1 \ldots \mathrm{d}\mathbf{r}_P \right. \\ &\qquad \left. + \sum_{\substack{i,j=1 \\ i \neq j}}^{P} \int_{\mathbb{R}^{3P}} \frac{1}{2|\mathbf{r}_i - \mathbf{r}_j|} |\psi((\mathbf{r}_1, s_1), \ldots, (\mathbf{r}_P, s_P))|^2 \, \mathrm{d}\mathbf{r}_1 \ldots \mathrm{d}\mathbf{r}_P \right. \end{aligned}$$

[1] The key point is that the invariance of $\nabla\Phi(\mathbf{X})$ assumed in the preceding section has to hold for all $\mathbf{X}$.

$$+\sum_{\ell=1}^{P}\int_{\mathbb{R}^{3P}} V(\mathbf{r}_\ell;\mathbf{x}_{1,1},\ldots,\mathbf{x}_{N,M})|\psi((\mathbf{r}_1,s_1),\ldots,(\mathbf{r}_P,s_P))|^2\,\mathrm{d}\mathbf{r}_1\ldots\mathrm{d}\mathbf{r}_P\Bigg)$$
$$+\frac{1}{2}\sum_{i,k=1}^{N}\sum_{\substack{j,m=1\\(j,m)\neq(i,k)}}^{M}\frac{Z^{(j)}Z^{(m)}}{|\mathbf{x}_{i,j}-\mathbf{x}_{k,m}|}. \tag{21}$$

Here, there are P electrons, with (possible) positions $(\mathbf{r}_1,\ldots,\mathbf{r}_P)\in\mathbb{R}^{3P}$ and spins $(s_1,\ldots,s_p)\in\{\pm 1/2\}^P$, and the interaction between ions and electrons is taken to be a Coulomb interaction:

$$V(\mathbf{r};\mathbf{x}_{1,1},\ldots,\mathbf{x}_{N,M})=-\sum_{i=1}^{N}\sum_{j=1}^{M}\frac{Z^{(j)}}{|\mathbf{r}-\mathbf{x}_{i,j}|}. \tag{22}$$

For a neutral system

$$P=N\sum_{j=1}^{M}Z^{(j)}. \tag{23}$$

Note the "min" in (21): we minimize out the wave function in order to get the ground state potential energy φ as a function of the parameters in the quantum mechanical energy. It is the invariance of this potential energy that we need. This invariance follows directly from its definition (21).

The invariance that follows from these definitions is

$$\begin{aligned}&\varphi(\mathbf{x}_{\Pi(1,1)},\ldots,\mathbf{x}_{\Pi(1,M)},\ldots,\mathbf{x}_{\Pi(N,1)},\ldots,\mathbf{x}_{\Pi(N,M)})\\&\quad=\varphi(\mathbf{x}_{1,1},\ldots,\mathbf{x}_{1,M},\ldots,\mathbf{x}_{N,1},\ldots,\mathbf{x}_{N,M})\\&\quad=\varphi(\mathbf{Q}\mathbf{x}_{1,1}+\mathbf{c},\ldots,\mathbf{Q}\mathbf{x}_{1,M}+\mathbf{c},\ldots,\mathbf{Q}\mathbf{x}_{N,1}+\mathbf{c},\ldots,\mathbf{Q}\mathbf{x}_{N,M}+\mathbf{c}),\end{aligned} \tag{24}$$

where Π is a permutation of $\{(1,1),\ldots,(N,M)\}$ that preserves atomic number: $(k,m)=\Pi(i,j)\Longrightarrow Z^{(m)}=Z^{(j)}$, and $\mathbf{Q}\in\mathrm{O}(3)$, $\mathbf{c}\in\mathbb{R}^3$. The proof of this invariance is straightforward. For example, for the EN term, using the form of V given above,

$$\begin{aligned}&\int_{\mathbb{R}^{3P}} V(\mathbf{r}_\ell;\mathbf{Q}\mathbf{x}_{1,1}+\mathbf{c},\ldots,\mathbf{Q}\mathbf{x}_{N,M}+\mathbf{c})|\psi((\mathbf{r}_1,s_1),\ldots,(\mathbf{r}_P,s_P))|^2\,\mathrm{d}\mathbf{r}_1\ldots\mathrm{d}\mathbf{r}_P\\&\quad=\int_{\mathbb{R}^{3P}} V(\mathbf{Q}^{\mathrm{T}}(\mathbf{r}_\ell-\mathbf{c});\mathbf{x}_{1,1},\ldots,\mathbf{x}_{N,M})\,|\psi((\mathbf{r}_1,s_1),\ldots,(\mathbf{r}_P,s_P))|^2\,\mathrm{d}\mathbf{r}_1\ldots\mathrm{d}\mathbf{r}_P\\&\quad=\int_{\mathbb{R}^{3P}} V(\hat{\mathbf{r}}_\ell;\mathbf{x}_{1,1},\ldots,\mathbf{x}_{N,M})\,|\psi((\mathbf{Q}\hat{\mathbf{r}}_1+\mathbf{c},s_1),\ldots,(\mathbf{Q}\hat{\mathbf{r}}_P+\mathbf{c},s_P))|^2\,|J|\,\mathrm{d}\hat{\mathbf{r}}_1\ldots\mathrm{d}\hat{\mathbf{r}}_P\\&\quad=\int_{\mathbb{R}^{3P}} V(\hat{\mathbf{r}}_\ell;\mathbf{x}_{1,1},\ldots,\mathbf{x}_{N,M})|\hat{\psi}((\hat{\mathbf{r}}_1,s_1),\ldots,(\hat{\mathbf{r}}_P,s_P))|^2\,\mathrm{d}\hat{\mathbf{r}}_1\ldots\mathrm{d}\hat{\mathbf{r}}_P,\end{aligned} \tag{25}$$

where J is the Jacobian of the transformation $(\hat{\mathbf{r}}_1,\ldots,\hat{\mathbf{r}}_P)\to(\mathbf{r}_1=\mathbf{Q}\hat{\mathbf{r}}_1+\mathbf{c},\ldots,\mathbf{r}_P=\mathbf{Q}\hat{\mathbf{r}}_P+\mathbf{c})$ and therefore $|J|=1$, and $\hat{\psi}$ is simply defined by

$$\hat{\psi}((\hat{\mathbf{r}}_1,s_1),\ldots,(\hat{\mathbf{r}}_P,s_P))=\psi((\mathbf{Q}\hat{\mathbf{r}}_1+\mathbf{c},s_1),\ldots,(\mathbf{Q}\hat{\mathbf{r}}_P+\mathbf{c},s_P)). \tag{26}$$

After changing variables in all the terms in the quantum mechanical energy, these terms retain their present form with $\hat{\psi}$ replacing ψ. From the definition (26) we note that $\hat{\psi}$ is antisymmetric and normalized, and therefore the minimization of the original energy over

wave functions ψ can be replaced by an equivalent minimization over wave functions $\hat{\psi}$, giving the same ground state energy and therefore proving the assertion. In physical terms $\hat{\psi}$ is just the wave function of the rotated[2] and translated state. The permutation invariance (under permutations of like species) of EN, as well as of NN, is obvious from the forms of these terms.

To get the force on atom (i,j) we take the negative derivative of the potential energy with respect to $\mathbf{x}_{i,j}$. Differentiating (24) with respect to $\mathbf{x}_{i,j}$, we get the invariance condition for forces:

$$-\frac{\partial\varphi}{\partial\mathbf{x}_{\Pi^{-1}(i,j)}}(\mathbf{x}_{\Pi(1,1)},\ldots,\mathbf{x}_{\Pi(1,M)},\ldots,\mathbf{x}_{\Pi(N,1)},\ldots,\mathbf{x}_{\Pi(N,M)})$$
$$=-\mathbf{Q}^{\mathrm{T}}\frac{\partial\varphi}{\partial\mathbf{x}_{i,j}}(\mathbf{Q}\mathbf{x}_{1,1}+\mathbf{c},\ldots,\mathbf{Q}\mathbf{x}_{1,M}+\mathbf{c},\ldots,\mathbf{Q}\mathbf{x}_{N,1}+\mathbf{c},\ldots,\mathbf{Q}\mathbf{x}_{N,M}+\mathbf{c}). \tag{27}$$

Now we discuss special issues that arise with infinite systems, $N=\infty$. Already from the formula (23), we see that infinite systems pose special problems, namely, that the energy, if not ill-defined, is at least infinite. However, one expects that under suitable hypotheses on the distribution of atoms that the force on an atom is nevertheless finite and has the invariance given in (27). In fact, the expectation is that under such hypotheses the actual value of the force is given by a formal[3] application of the Hellmann–Feynman formula, which exhibits the invariance (27). The type of argument that is expected to give these results is the following: take the energy difference between a structure with one atom displaced and the perfect structure, both structures cutoff by the same ball so the energies are finite, then pass to the large-body limit by letting the radius of the ball go to infinity, and finally pass to the limit in the difference quotient to get the force. To our knowledge, there is no rigorous argument of this type in full quantum mechanics. However, it is widely believed that the consequence of such an argument would be a finite force with the invariance properties given in (27). In any case we shall assume that the invariance condition on forces is (27), which is required to hold independently for all $\mathbf{Q}\in\mathrm{O}(3)$, $\mathbf{c}\in\mathbb{R}^3$, permutations Π that preserve species, and all arguments $(\mathbf{x}_{1,1},\ldots,\mathbf{x}_{N,M})$ in a domain $\mathscr{I}$, which itself is invariant under these transformations.

Now we identify the group action more explicitly. Let the isometry group of the structure be $\mathscr{G}$ defined by (9): $(\mathbf{Q}|\mathbf{c})\in\mathscr{G}\Longrightarrow\mathbf{Q}\mathbf{x}_{i,j}+\mathbf{c}=\mathbf{x}_{\Pi(i,j)}$, where Π is a permutation of $\{(i,j): i=1,\ldots,N,\ j=1,\ldots,M\}$ that preserves species. The use of the permutation Π is just a shorthand way of saying that this transformation restores the structure. Accounting for the invariance of the forces (27), the group actions that make the argument given in Section 3.1 work are (recall $\mathbf{X}=\mathbf{x}_{i,j}, i=1,\ldots,N,\ j=1,\ldots,M$):

$$(\mathbf{T}\mathbf{X})_{i,j}=\mathbf{Q}\mathbf{x}_{\Pi^{-1}(i,j)}+\mathbf{c},\quad(\mathbf{T}'\mathbf{X})_{i,j}=\mathbf{Q}\mathbf{x}_{\Pi^{-1}(i,j)}. \tag{28}$$

With these definitions we see that the invariance condition $\nabla\Phi(\mathbf{T}\mathbf{X})=\mathbf{T}'\nabla\Phi(\mathbf{X})$ assumed in (14) is verified by (27). Also, using the species invariance of Π, the mass matrix satisfies the invariance condition $\mathbf{T}'\mathbf{M}(\mathbf{T}')^{-1}=\mathbf{M}$. This, together with sufficient smoothness of $\partial\phi/\partial\mathbf{x}_{i,j}$ that insures a unique solution of the equations of molecular dynamics, verifies the

[2]Though in fact, as noted, $\mathbf{Q}$ can belong to the full orthogonal group.

[3]The usual derivation of the Hellmann–Feynman formula is valid only for finite systems.

hypotheses of Section 3.1. The conclusion is $\mathbf{TX}(t) = \mathbf{X}(t)$, which explicitly is

$$\mathbf{Q}\mathbf{x}_{i,j}(t) + \mathbf{c} = \mathbf{x}_{\Pi(i,j)}(t). \tag{29}$$

In principle, this gives the mapping between atoms of the structure that ensures an exact solution of the equations of molecular dynamics. Depending on the choice of the subgroup of the isometry group, this gives effectively a reduction of the system, typically from infinite to finite. Roughly speaking, a large subgroup will imply that the simulation will be highly constrained but the motions of only a few atoms will need to be simulated. A smaller subgroup will allow more simulated atoms, but perhaps a more representative simulation in terms of properties of the structure.

All this is rather abstract. To see exactly what are these groups and to understand more clearly what really one needs to do in an actual simulation, we specialize these conditions of invariance to the formulas for objective structures. We do this separately in the atomic (where the formulas are particularly simple) and molecular cases.

3.3. Three-term formula: atomic case

We consider the three-term formula (7) in the atomic case, $M = 1$, and we drop the second index, $\mathbf{x}_i = \mathbf{x}_{i,1},\ i = 1, \ldots, N$. Recall that in the three-term formula we also replace the indexing set $\{1, \ldots, N\}$ by $\mathbb{Z}^3$ and use (p, q, r) in place of i. The atomic positions for an objective atomic structure are

$$\mathbf{x}_{p,q,r} = \mathbf{x}_1 + \sum_{i=0}^{p-1} \mathbf{R}_3^i \mathbf{t}_3 + \mathbf{R}_3^p \sum_{j=0}^{q-1} \mathbf{R}_2^j \mathbf{t}_2 + \mathbf{R}_3^p \mathbf{R}_2^q \sum_{k=0}^{r-1} \mathbf{R}_1^k \mathbf{t}_1, \tag{30}$$

where $\mathbf{R}_1, \mathbf{R}_2, \mathbf{R}_3 \in \mathrm{O}(3)$ and $\mathbf{t}_1, \mathbf{t}_2, \mathbf{t}_3 \in \mathbb{R}^3$ satisfy the restrictions:

$$\begin{aligned} &\mathbf{t}_3 + \mathbf{R}_3\mathbf{t}_2 = \mathbf{t}_2 + \mathbf{R}_2\mathbf{t}_3, \quad \mathbf{R}_3\mathbf{R}_2 = \mathbf{R}_2\mathbf{R}_3, \\ &\mathbf{t}_3 + \mathbf{R}_3\mathbf{t}_1 = \mathbf{t}_1 + \mathbf{R}_1\mathbf{t}_3, \quad \mathbf{R}_3\mathbf{R}_1 = \mathbf{R}_1\mathbf{R}_3, \\ &\mathbf{t}_2 + \mathbf{R}_2\mathbf{t}_1 = \mathbf{t}_1 + \mathbf{R}_1\mathbf{t}_2, \quad \mathbf{R}_2\mathbf{R}_1 = \mathbf{R}_1\mathbf{R}_2, \end{aligned} \tag{31}$$

and $\mathbf{x}_1 \in \mathbb{R}^3$. Under these restrictions the formula (31) always generates an objective atomic structure. That is, if we put $\mathbf{R}_{p,q,r} = \mathbf{R}_3^p \mathbf{R}_2^q \mathbf{R}_1^r$ then

$$\mathbf{x}_{p,q,r} + \mathbf{R}_{p,q,r}(\mathbf{x}_{j,k,l} - \mathbf{x}_{0,0,0}) = \mathbf{x}_{p+j,q+k,r+l}. \tag{32}$$

It is again worth noting that this family of structures helps us understand what structure is being simulated; for the argument itself, we are merely using it to generate an appropriate group.

Thus, we extract some isometry groups of this family of structures. An isometry group that generates the full structure when applied to a single atomic position will give a highly constrained[4] simulation, having only one atom in the fundamental domain, so what is desired is a good collection of subgroups that allow a broad set of fundamental domains containing various numbers of atoms. We have noted in (10), or one can see immediately from (32), that the following orthogonal transformations and translations restore the full structure $\mathscr{S} = \{\mathbf{x}_{p,q,r} : (p, q, r) \in \mathbb{Z}^3\}$:

$$\mathbf{Q}\mathscr{S} + \mathbf{c} = \mathscr{S}, \tag{33}$$

[4]Though not necessarily trivial; for a carbon nanotube, the radius could oscillate uniformly.

where

$$\mathbf{Q}=\mathbf{Q}_{p,q,r}=\mathbf{R}_3^p\mathbf{R}_2^q\mathbf{R}_1^r,\quad \mathbf{c}=\mathbf{c}_{p,q,r}=\sum_{i=0}^{p-1}\mathbf{R}_3^i\mathbf{t}_3+\mathbf{R}_3^p\sum_{j=0}^{q-1}\mathbf{R}_2^j\mathbf{t}_2 + \mathbf{R}_3^p\mathbf{R}_2^q\sum_{k=0}^{r-1}\mathbf{R}_1^k\mathbf{t}_1-\mathbf{R}_3^p\mathbf{R}_2^q\mathbf{R}_1^r\mathbf{x}_1. \tag{34}$$

These transformations form a group under the usual operations $(\mathbf{Q}_2|\mathbf{c}_2)\circ(\mathbf{Q}_1|\mathbf{c}_1)=(\mathbf{Q}_2\mathbf{Q}_1|\mathbf{Q}_2\mathbf{c}_1+\mathbf{c}_2)$.

We extend the notation by letting $v=(i,j,k)\in\mathbb{Z}^3$ and $\eta=(p,q,r)\in\mathbb{Z}^3$. A very useful family of subgroups of the group defined by (34) is obtained by taking $\mu=\mu_i^j$ to be a fixed 3×3 invertible matrix of integers and defining the subgroup by restricting $(\mathbf{Q}_\eta,\mathbf{c}_\eta)$ in (34) to the values $\eta^j=\mu_i^j\xi^i$, where $\xi\in\mathbb{Z}^3$. After some calculation it is seen that this does give a subgroup. We note that, if we think of the triple of integers as generating a Bravais lattice via the usual formula $\eta^j\mathbf{e}_j=p\mathbf{e}_1+q\mathbf{e}_2+r\mathbf{e}_3$, the choice $\eta^j=\mu_i^j\xi^i$ is exactly the method of assigning the subgroup in periodic molecular dynamics for this lattice. Thus this method of assigning the subgroup exactly maps the periodic MD problem to the objective MD problem. In both cases $|\det\mu|\geqslant 1$ is the number of atoms in the fundamental domain, and therefore the number of atoms effectively being simulated. See, however, the remark at the end of this section.

Now we give some detail on the invariance conditions for these subgroups, following the notation of Sections 3.1 and 3.2. For these subgroups the permutation of (28) is $\Pi(v)=v+\eta$, $\eta^j=\mu_i^j\xi^i$, $\xi\in\mathbb{Z}^3$. The invariance condition (27) on the forces becomes

$$\begin{aligned}&-\frac{\partial\varphi}{\partial\mathbf{x}_{v-\eta}}(\ldots,\mathbf{x}_{v_1},\mathbf{x}_{v_2},\ldots,\mathbf{x}_{v_N},\ldots)\\&\quad=-\mathbf{Q}_\eta^{\mathrm{T}}\frac{\partial\varphi}{\partial\mathbf{x}_v}(\ldots,\mathbf{Q}_\eta\mathbf{x}_{v_1-\eta}+\mathbf{c}_\eta,\mathbf{Q}_\eta\mathbf{x}_{v_2-\eta}+\mathbf{c}_\eta,\ldots,\mathbf{Q}_\eta\mathbf{x}_{v_N-\eta}+\mathbf{c}_\eta,\ldots).\end{aligned} \tag{35}$$

The final invariance condition on the solution is

$$\mathbf{x}_{v+\eta}(t)=\mathbf{Q}_\eta\mathbf{x}_v(t)+\mathbf{c}_\eta, \tag{36}$$

which holds for all $t\in[0,T)$, all $v=(i,j,k)\in\mathbb{Z}^3$, and all $\eta=(p,q,r)$ of the form $\eta^j=\mu_i^j\xi^i$ where $\xi\in\mathbb{Z}^3$.

To do an objective MD simulation in this format, consider triples of integers (i,j,k) that lie in the set

$$\mathscr{I}=\left\{\lambda_1\mu_1^j+\lambda_2\mu_2^j+\lambda_3\mu_3^j:\sum\lambda_i\leqslant 1,\ 0\leqslant\lambda_i<1\right\}\cap\mathbb{Z}^3. \tag{37}$$

These are triples of integers in a parallelpiped defined by the vectors $(\mu_1^j,\mu_2^j,\mu_3^j)$ and there are $|\det\mu|$ of them. Assign the initial positions and velocities of the atoms $\mathbf{x}_v$, $v\in\mathscr{I}$, in any way. Construct other atoms in the structure by applying the formula (36) to $v\in\mathscr{I}$ and all η as given there. The atoms that are directly simulated are only $\mathbf{x}_v$, $v\in\mathscr{I}$, but forces on these atoms are calculated using all other atoms of the structure. If the forces have a cutoff, only atomic positions corresponding to a restricted set of η in (36) need to be calculated, i.e., only those whose positions fall within the cutoff. At each timestep the positions of the atoms not being simulated need to be updated using (36). The group, i.e., the matrices $\mathbf{Q}_\eta$ and $\mathbf{c}_\eta$, must remain fixed during the course of the simulation.

We conclude this section by echoing the warning given two paragraphs after (8). That is, the three-term formula sometimes gives structures that are not discrete.[5] Strictly speaking, the structures generated are still objective structures (because (32) holds), but the molecular dynamics fails. The point of failure of the argument is at the end of the paragraph following (27), because the potential typically has a singularity when two atoms approach each other. Thus it is important to enforce discreteness of the structure. We show how to do this in the case of carbon nanotubes, but we do not yet have a complete understanding of the conditions for discreteness in the general case.

3.4. Three-term formula: molecular case

Now we very briefly outline the objective molecular case. The underlying structure is now given by

$$\mathbf{x}_{(p,q,r),k} = \sum_{i=0}^{p-1} \mathbf{R}_3^i \mathbf{t}_3 + \mathbf{R}_3^p \sum_{j=0}^{q-1} \mathbf{R}_2^j \mathbf{t}_2 + \mathbf{R}_3^p \mathbf{R}_2^q \sum_{k=0}^{r-1} \mathbf{R}_1^k \mathbf{t}_1 + \mathbf{x}_1 + \mathbf{R}_{p,q,r} \mathbf{p}_k, \tag{38}$$

where $\mathbf{R}_1, \mathbf{R}_2, \mathbf{R}_3 \in \mathrm{O}(3)$ and $\mathbf{t}_1, \mathbf{t}_2, \mathbf{t}_3 \in \mathbb{R}^3$ satisfy the restrictions:

$$\begin{aligned} &\mathbf{t}_3 + \mathbf{R}_3\mathbf{t}_2 = \mathbf{t}_2 + \mathbf{R}_2\mathbf{t}_3, \quad \mathbf{R}_3\mathbf{R}_2 = \mathbf{R}_2\mathbf{R}_3, \\ &\mathbf{t}_3 + \mathbf{R}_3\mathbf{t}_1 = \mathbf{t}_1 + \mathbf{R}_1\mathbf{t}_3, \quad \mathbf{R}_3\mathbf{R}_1 = \mathbf{R}_1\mathbf{R}_3, \\ &\mathbf{t}_2 + \mathbf{R}_2\mathbf{t}_1 = \mathbf{t}_1 + \mathbf{R}_1\mathbf{t}_2, \quad \mathbf{R}_2\mathbf{R}_1 = \mathbf{R}_1\mathbf{R}_2, \end{aligned} \tag{39}$$

$\mathbf{x}_1 \in \mathbb{R}^3$, $\mathbf{R}_{p,q,r} = \mathbf{R}_3^p \mathbf{R}_2^q \mathbf{R}_1^r$, and $\{\mathbf{x}_1 + \mathbf{p}_1, \ldots, \mathbf{x}_1 + \mathbf{p}_M\}$ are the positions of atoms within molecule $(0,0,0)$. Under these restrictions the formula (31) always generates an objective molecular structure. That is, if we put $\mathbf{R}_{p,q,r} = \mathbf{R}_3^p \mathbf{R}_2^q \mathbf{R}_1^r$ then

$$\mathbf{x}_{(p,q,r),k} + \mathbf{R}_{p,q,r}(\mathbf{x}_{(j,k,l),\ell} - \mathbf{x}_{(0,0,0),k}) = \mathbf{x}_{(p+j,q+k,r+l),\ell}. \tag{40}$$

As we have noted above (and as can be seen directly from (40)), the following orthogonal transformations and translations restore the full structure $\mathscr{S} = \{\mathbf{x}_{p,q,r} : p, q, r \in \mathbb{Z}\}$:

$$\mathbf{Q}\mathscr{S} + \mathbf{c} = \mathscr{S}, \tag{41}$$

where

$$\begin{aligned} \mathbf{Q} = \mathbf{Q}_{p,q,r} = \mathbf{R}_3^p \mathbf{R}_2^q \mathbf{R}_1^r, \quad \mathbf{c} = \mathbf{c}_{p,q,r} = &\sum_{i=0}^{p-1} \mathbf{R}_3^i \mathbf{t}_3 + \mathbf{R}_3^p \sum_{j=0}^{q-1} \mathbf{R}_2^j \mathbf{t}_2 \\ &+ \mathbf{R}_3^p \mathbf{R}_2^q \sum_{k=0}^{r-1} \mathbf{R}_1^k \mathbf{t}_1 - \mathbf{R}_3^p \mathbf{R}_2^q \mathbf{R}_1^r \mathbf{x}_1. \end{aligned} \tag{42}$$

Note the interesting fact that even in the objective molecular case, the transformations $(\mathbf{Q}|\mathbf{c})$ depend on the choice of molecule, but not on the atom within the molecule (see James, 2006).

[5] If one wants to understand intuitively how a failure of discreteness can occur, note that the three-term formula in a very special case ($\mathbf{R}_1 = \mathbf{R}_2 = \mathbf{R}_3 = \mathbf{I}, \mathbf{t}_1 = 0, \mathbf{t}_3 = (1/\alpha)\mathbf{t}_2 = \mathbf{t}$) is $(p + \alpha q)\mathbf{t}$. If α is irrational and p and q are chosen to be suitable large negative and positive integers, respectively, one sees that this formula produces denser and denser arrays of atomic position near the origin.

As above, let $v=(i,j,k)\in\mathbb{Z}^3$ and $\eta=(p,q,r)\in\mathbb{Z}^3$ represent triples of integers. Let $\mu=\mu_i^j$ be a fixed 3×3 invertible matrix of integers. The subgroups of interest are obtained by restricting $(\mathbf{Q}_\eta,\mathbf{c}_\eta)$ in (42) to the values $\eta^j=\mu_i^j\xi^i$, where $\xi\in\mathbb{Z}^3$.

For these subgroups the permutation of (28) is $\Pi(v)=v+\eta$, $\eta^j=\mu_i^j\xi^i$, $\xi\in\mathbb{Z}^3$, as in the atomic case. The invariance condition (27) on the forces is

$$\begin{aligned}&-\frac{\partial\varphi}{\partial\mathbf{x}_{v-\eta,k}}(\ldots,\mathbf{x}_{v_1,1},\ldots,\mathbf{x}_{v_1,M},\ldots,\mathbf{x}_{v_N,1},\ldots,\mathbf{x}_{v_N,M},\ldots)\\&\quad=-\mathbf{Q}_\eta^{\mathrm{T}}\frac{\partial\varphi}{\partial\mathbf{x}_{v,k}}(\ldots,\mathbf{Q}_\eta\mathbf{x}_{v_1-\eta,1}+\mathbf{c}_\eta,\ldots,\mathbf{Q}_\eta\mathbf{x}_{v_1-\eta,M}+\mathbf{c}_\eta,\ldots,\mathbf{Q}_\eta\mathbf{x}_{v_N-\eta,1}\\&\quad+\mathbf{c}_\eta,\ldots,\mathbf{Q}_\eta\mathbf{x}_{v_N-\eta,M}+\mathbf{c}_\eta,\ldots).\end{aligned}\tag{43}$$

The final invariance condition on the solution is

$$\mathbf{x}_{v+\eta,k}(t)=\mathbf{Q}_\eta\mathbf{x}_{v,k}(t)+\mathbf{c}_\eta,\tag{44}$$

which holds for all $t\in[0,T)$, all $v=(i,j,k)\in\mathbb{Z}^3$, and all $\eta=(p,q,r)$ of the form $\eta^j=\mu_i^j\xi^i$ for some $\xi\in\mathbb{Z}^3$.

To set up the simulation one follows the procedure given above for the objective atomic case; it is only necessary, for each value of $v\in\mathscr{I}$ to add to the simulation the M position vectors $\mathbf{p}_1,\ldots,\mathbf{p}_M$ whose initial positions and velocities can be arbitrarily assigned.

3.5. Case of the finite groups

This case is simple. Recall that a finite subgroup $\mathscr{G}=\{\mathbf{Q}_1,\ldots,\mathbf{Q}_N\}$ of O(3) is assigned, $\mathbf{Q}_1=\mathbf{I}$, and the structures are given by $\mathscr{S}=\{\mathbf{x}_{i,j}=\mathbf{Q}_i(\mathbf{y}_1+\mathbf{p}_j):i=1,\ldots,N,\ j=1,\ldots,M,\ \mathbf{y}_1\in\mathbb{R}^3\}$. Let $\Pi^{(i)}(k)$, $k=1,\ldots,N$ be a permutation of $\{1,\ldots,N\}$ associated to the multiplication table of the group $\mathscr{G}$, that is, $\Pi^{(i)}(k)=\ell$ if $\mathbf{Q}_i\mathbf{Q}_k=\mathbf{Q}_\ell$. Then an easy calculation yields

$$\mathbf{x}_{i,j}+\mathbf{Q}_i(\mathbf{x}_{k,m}-\mathbf{x}_{1,j})=\mathbf{x}_{\Pi^{(i)}(k),m},\tag{45}$$

and also

$$\mathbf{Q}\mathscr{S}+\mathbf{c}=\mathscr{S},\tag{46}$$

where $\mathbf{Q}=\mathbf{Q}_i,\mathbf{c}=0$. The permutation appearing in (28) associated to a group element i is simply $\Pi(m,k)=(\Pi^{(i)}(m),k)$. The invariance condition (27) on the forces is

$$\begin{aligned}&-\frac{\partial\varphi}{\partial\mathbf{x}_{(\Pi^{(\ell)})^{-1}(i),j}}(\mathbf{x}_{\Pi^{(\ell)}(1),1},\ldots,\mathbf{x}_{\Pi^{(\ell)}(1),M},\ldots,\mathbf{x}_{\Pi^{(\ell)}(N),1},\ldots,\mathbf{x}_{\Pi^{(\ell)}(N),M})\\&\quad=-\mathbf{Q}_\ell^{\mathrm{T}}\frac{\partial\varphi}{\partial\mathbf{x}_{i,j}}(\mathbf{Q}_\ell\mathbf{x}_{1,1},\ldots,\mathbf{Q}_\ell\mathbf{x}_{1,M},\ldots,\mathbf{Q}_\ell\mathbf{x}_{N,1},\ldots,\mathbf{Q}_\ell\mathbf{x}_{N,M})\end{aligned}\tag{47}$$

(no sum over ℓ). The final invariance condition on the solution is

$$\mathbf{x}_{\Pi^{(\ell)}(i),j}(t)=\mathbf{Q}_\ell\,\mathbf{x}_{i,j}(t),\tag{48}$$

which holds for all $t\in[0,T)$, all $i,\ell=1,\ldots,N$, and all $j=1,\ldots,M$.

4. Example: single-walled carbon nanotubes

4.1. Single-walled carbon nanotubes in the hexagon-lattice nomenclature

The structure of carbon nanotubes is commonly specified in the literature in terms of indices n and m. In the unrolled representation, these indices represent the components of the circular circumference vector $\mathbf{c}$ of the nanotube on the lattice vectors $\mathbf{a}$ and $\mathbf{b}$ of the honeycomb lattice, i.e., $\mathbf{c} = n\mathbf{a} + m\mathbf{b}$. By convention, the lattice vectors $\mathbf{a}$ and $\mathbf{b}$ are the particular ones shown in Fig. 2. After rolling into the shape of the carbon nanotube, $\mathbf{c}$ is mapped to a circular circumference on the nanotube. The chirality or wrapping index is measured by the angle χ enclosed by $\mathbf{c}$ and the lattice vector $\mathbf{a}$. The special cases corresponding to $(n, 0)$ and (n, n) are called zigzag and armchair configurations, respectively.

Given (n, m) the formula for the position vectors of atoms on the nanotube is

$$\mathbf{y}(p, q) = r\cos(2\pi\xi(p, q))\,\mathbf{e}_1 + r\sin(2\pi\xi(p, q))\,\mathbf{e}_2 + \eta(p, q)\,\mathbf{e}_3, \tag{49}$$

where $\mathbf{e}_1, \mathbf{e}_2, \mathbf{e}_3$ is an orthonormal basis, $\mathbf{e}_3$ being on the axis of the nanotube, and

$$\begin{aligned} r &= \frac{\sqrt{3}\,l_{\mathrm{C-C}}}{2\pi}\sqrt{n^2 + m^2 + nm}, \\ \xi(p, q) &= \frac{(2n + m)p + (2m + n)q}{2(n^2 + m^2 + nm)}, \\ \eta(p, q) &= \frac{3l_{\mathrm{C-C}}(pm - qn)}{2\sqrt{n^2 + m^2 + nm}}. \end{aligned} \tag{50}$$

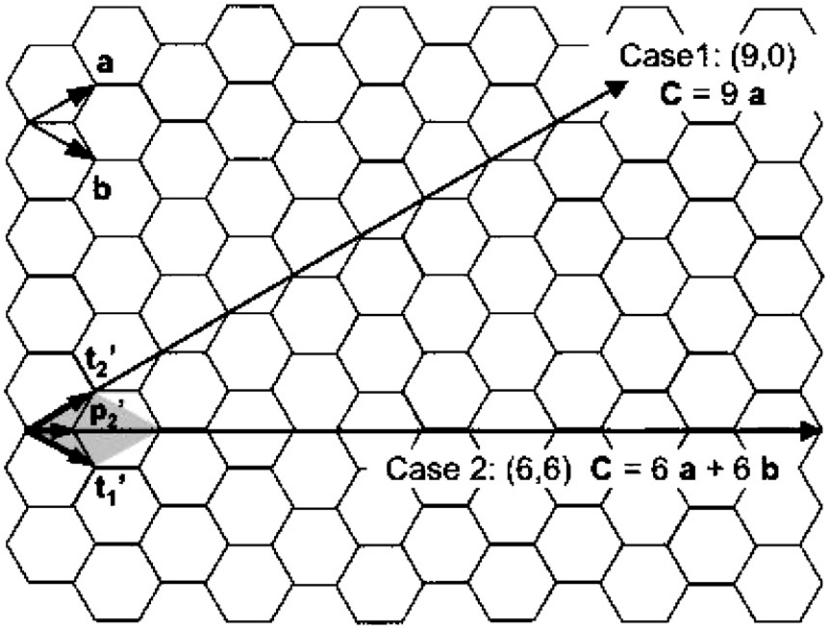

Fig. 2. The two carbon nanotubes discussed in Cases 1 and 2 are specified on a graphene sheet by the vector $\mathbf{c}$, which is mapped onto the nanotube's circumference. The vectors $\mathbf{t}_1', \mathbf{t}_2', \mathbf{p}_2'$ are mapped by (49) onto the vectors $\mathbf{t}_1, \mathbf{t}_2, \mathbf{p}_2$ used in the objective description of the nanotube. Shaded area corresponds to the primitive fundamental domain.

Here, l_{C-C} is the bond length on the sheet before rolling. To get the positions of all the atoms on the nanotube, one evaluates (49), (50) at the arguments (p,q) and $(p+1/3, q+1/3)$ where (p,q) runs over all pairs of integers. The position vectors $\mathbf{y}(p,q)$ and $\mathbf{y}(p+1/3, q+1/3)$ represent the positions of atoms that were at positions $p\mathbf{a}+q\mathbf{b}$ and $(p+1/3)\mathbf{a}+(q+1/3)\mathbf{b}$, respectively, before rolling. The two positions $\mathbf{y}(p,q)$ and $\mathbf{y}(p+1/3, q+1/3)$ can be taken as the coordinates of each two-atom molecule in the sense of objective structures.

The mapping (49), (50) describes an exact isometric mapping of the graphene sheet shown in Fig. 2. Due to finite curvature effects, the bond lengths of atoms will be slightly changed upon rolling. This can be compensated for by scaling r and η appropriately; in the actual physical case the equilibrium bond lengths will anyway be slightly different from those of a graphene sheet. This will not matter for objective molecular dynamics of nanotubes, because this dynamics allows relaxation of the radius. However, as we explain below, the twist and extension of a carbon nanotube can be prescribed in objective molecular dynamics.

In conjunction with Fig. 2, we will implement the theory on two kinds of nanotubes.

1. Case 1: $n=9,\ m=0$. In this case $\mathbf{c}=9\mathbf{a}$ and the chiral angle $\chi=0$.
2. Case 2: $n=6,\ m=6$. In this case $\mathbf{c}=6\mathbf{a}+6\mathbf{b}$ and the chiral angle $\chi=\pi/6$.

4.2. Carbon nanotubes as objective molecular structures

Single-walled carbon nanotubes are objective molecular structures in which the molecule contains two carbon atoms. We will show that they are given by the two-term formula, that is,

$$\mathbf{x}_{(p,q),k}=\mathbf{x}_1+\sum_{i=0}^{p-1}\mathbf{R}_2^i\mathbf{t}_2+\mathbf{R}_2^p\sum_{i=0}^{q-1}\mathbf{R}_1^i\mathbf{t}_1+\mathbf{R}_2^p\mathbf{R}_1^q\mathbf{p}_k,\quad k=1,2, \tag{51}$$

where p,q are integers, $\mathbf{R}_1,\mathbf{R}_2\in \mathrm{O}(3)$ and $\mathbf{t}_1,\mathbf{t}_2\in\mathbb{R}^3$, satisfy the restrictions

$$(\mathbf{R}_2-\mathbf{I})\mathbf{t}_1=(\mathbf{R}_1-\mathbf{I})\mathbf{t}_2,\quad \mathbf{R}_1\mathbf{R}_2=\mathbf{R}_2\mathbf{R}_1 \tag{52}$$

We will use the notation

$$\mathbf{Q}_\theta=\begin{pmatrix}\cos\theta & -\sin\theta & 0\\ \sin\theta & \cos\theta & 0\\ 0 & 0 & 1\end{pmatrix}, \tag{53}$$

and all components here and below are expressed in the same orthonormal basis $(\mathbf{e}_1,\mathbf{e}_2,\mathbf{e}_3)$ and in all cases $\mathbf{R}_1=\mathbf{Q}_{\theta_1},\mathbf{R}_2=\mathbf{Q}_{\theta_2}$. Since coaxial rotation matrices commute, the second condition of (52) holds. When the orthogonal matrices $\mathbf{R}_1$ and $\mathbf{R}_2$ have these simple coaxial forms, the formula (51) also has a simpler alternative form that will be useful. To derive this form, decompose $\mathbf{t}_1=\tau_1\mathbf{e}_3+\mathbf{r}_1$ and $\mathbf{t}_2=\tau_2\mathbf{e}_3+\mathbf{r}_2$, where $\mathbf{r}_1\cdot\mathbf{e}_3=\mathbf{r}_2\cdot\mathbf{e}_3=0$. Considering only $\mathbf{t}_1$ ($\mathbf{t}_2$ is similar) we choose $\mathbf{s}_1\cdot\mathbf{e}_3=0$ to satisfy $(\mathbf{R}_1-\mathbf{I})\mathbf{s}_1=\mathbf{r}_1$ (this can always be done if $\theta_1\neq 0$). Now iterate the formula $\mathbf{R}_1\mathbf{s}_1-\mathbf{s}_1=\mathbf{r}_1$ to get

$$\mathbf{R}_1^q\mathbf{s}_1=\mathbf{s}_1+\sum_{j=0}^{q-1}\mathbf{R}_1^j\mathbf{r}_1. \tag{54}$$

Note also that

$$\sum_{j=0}^{q-1} \mathbf{R}_1^j(\tau_1 \mathbf{e}_3) = q\tau_1 \mathbf{e}_3. \tag{55}$$

Now substitute $\mathbf{t}_1 = \tau_1 \mathbf{e}_3 + \mathbf{r}_1$ and $\mathbf{t}_2 = \tau_2 \mathbf{e}_3 + \mathbf{r}_2$ into (51) and use (54) and (55), and their analogs for $\mathbf{t}_2$, and also note that the compatibility condition $(\mathbf{R}_2 - \mathbf{I})\mathbf{t}_1 = (\mathbf{R}_1 - \mathbf{I})\mathbf{t}_2$ becomes simply $\mathbf{s}_1 = \mathbf{s}_2$. Calling $\mathbf{s} = \mathbf{s}_1 = \mathbf{s}_2$, we conclude that the two-term formula (51) in this case is equivalent to[6]

$$\mathbf{x}_{(p,q),k} = \mathbf{x}_1 - \mathbf{s} + \mathbf{R}_2^p \mathbf{R}_1^q(\mathbf{s} + \mathbf{p}_k) + (p\tau_2 + q\tau_1)\mathbf{e}_3, \quad k = 1, 2. \tag{56}$$

Note that, since $\mathbf{e}_3$ is the axis of $\mathbf{R}_{1,2}$ this formula can be interpreted as applying successive commuting screw transformations $(\mathbf{R}_2^p | p\tau_2) \circ (\mathbf{R}_1^q | q\tau_1)$ to the two-atom basis $\mathbf{s} + \mathbf{p}_{1,2}$, as noticed before in White et al. (1993) and Popov (2004).

But now by comparing (56) to (49) we see that we have proved that any (n, m)-carbon nanotube is an objective molecular structure given by the two-term formula. That is, first we put $\mathbf{x}_1 = \mathbf{s}$ in (56) so that the centerline of the tube is the three-axis as in the formula (49). Then, using the coaxiality of $\mathbf{R}_1$ and $\mathbf{R}_2$, we have that $\mathbf{R}_2^p \mathbf{R}_1^q = \mathbf{Q}_{p\theta_2 + q\theta_1}$. Thus, we can take $\mathbf{p}_1 = 0$ and $\mathbf{s} = r\mathbf{e}_1$ and (56) reduces exactly to (49) evaluated at integers (p, q), where

$$\theta_2 = 2\pi\xi(1, 0) = \frac{\pi(2n + m)}{n^2 + m^2 + nm}, \quad \theta_1 = 2\pi\xi(0, 1) = \frac{\pi(2m + n)}{n^2 + m^2 + nm} \tag{57}$$

and

$$\tau_2 = \eta(1, 0) = \frac{3m\, l_{\mathrm{C-C}}}{2\sqrt{n^2 + m^2 + nm}}, \quad \tau_1 = \eta(0, 1) = \frac{-3nl_{\mathrm{C-C}}}{2\sqrt{n^2 + m^2 + nm}}. \tag{58}$$

The remaining points, formula (49) at $(p + 1/3, q + 1/3)$, are obtained by an appropriate choice of $\mathbf{p}_2$. That is, by trigonometric identities,

$$\begin{aligned} & r\cos(2\pi\xi(p + 1/3, q + 1/3))\mathbf{e}_1 + r\sin(2\pi\xi(p + 1/3, q + 1/3))\mathbf{e}_2 \\ & \quad = r\cos(2\pi(\xi(p, q) + \xi(1/3, 1/3))\mathbf{e}_1 + r\sin(2\pi\xi(p, q) + \xi(1/3, 1/3))\mathbf{e}_2 \\ & \quad = r[\cos 2\pi\xi(1/3, 1/3)\mathbf{e}_1 + \sin 2\pi\xi(1/3, 1/3)\mathbf{e}_2]\cos(2\pi(\xi(p, q)) \\ & \qquad + r[-\sin 2\pi\xi(1/3, 1/3)\mathbf{e}_1 + \cos 2\pi\xi(1/3, 1/3)\mathbf{e}_2]\sin(2\pi\xi(p, q)). \end{aligned} \tag{59}$$

Thus we have exact agreement of (49) at $(p + 1/3, q + 1/3)$ and (56) at (p, q) and $k = 2$ if we choose

$$\begin{aligned} \mathbf{p}_2 &= r\cos(2\pi\xi(1/3, 1/3))\mathbf{e}_1 + r\sin(2\pi\xi(1/3, 1/3))\mathbf{e}_2 + \eta(1/3, 1/3)\mathbf{e}_3 - \mathbf{s} \\ &= \mathbf{y}(1/3, 1/3) - \mathbf{y}(0, 0). \end{aligned} \tag{60}$$

Obviously, there is some freedom in the choice of $\mathbf{s}, \mathbf{p}_1, \mathbf{p}_2$ in the formula (56) for the description of a given nanotube. For example, one can replace $\mathbf{s}$ by $\mathbf{s} + \mathbf{c}$ and correspondingly change $\mathbf{p}_k$ to $\mathbf{p}_k - \mathbf{c}$, $k = 1, 2$, without changing the atomic positions. In fact, this freedom can be used to make $\mathbf{s} = 0$, so that $\mathbf{t}_1$ and $\mathbf{t}_2$ are conveniently both parallel to $\mathbf{e}_3$.

[6]The reason for not writing the two-term formula in this simplified way originally is that the formulas (51), (52) describe objective molecular structures that are not describable by (56).

In summary, carbon nanotubes of any chirality (n,m) are objective atomic structures given by the two-term formula (51) with a two-atom molecule. The values of $\mathbf{R}_{1,2}$ are given by (53) with $\theta=\theta_{1,2}$ given in (57), $\mathbf{t}_{1,2}=\tau_{1,2}+(\mathbf{R}_{1,2}-\mathbf{I})\mathbf{s}$ with $\mathbf{s}=r\mathbf{e}_1$ and $\tau_{1,2}$ given in (58), $\mathbf{p}_1=0$ and $\mathbf{p}_2$ is given by (60). There is the additional freedom of simultaneously changing $\mathbf{s}\to\mathbf{s}+\mathbf{c}$, and $\mathbf{p}_k\to\mathbf{p}_k-\mathbf{c}$ without affecting the atomic positions.

In fact, in the specific examples below we will take advantage of this additional freedom to make $\mathbf{t}_{1,2}$ parallel to $\mathbf{e}_3$, by assigning $\mathbf{c}=-\mathbf{s}=-\mathbf{y}(0,0)$. In this case we have

$$\mathbf{p}_1=\mathbf{y}(0,0),\quad \mathbf{p}_2=\mathbf{y}(1/3,1/3), \tag{61}$$

and

$$\mathbf{t}_2=\eta(1,0)\mathbf{e}_3=\frac{3ml_{\mathrm{C-C}}}{2\sqrt{n^2+m^2+nm}}\mathbf{e}_3,\quad \mathbf{t}_1=\eta(0,1)\mathbf{e}_3=\frac{-3nl_{\mathrm{C-C}}}{2\sqrt{n^2+m^2+nm}}\mathbf{e}_3. \tag{62}$$

In the two nanotube cases given in the preceding section, taking $l_{\mathrm{C-C}}=1.42\,\text{Å}$ we have:

1. Case 1 $(n=9,m=0)$. $\theta_2=2\pi/9,\theta_1=\pi/9$, $\mathbf{t}_2=0,\mathbf{t}_1=(0,0,-2.13)\text{Å}$, $\mathbf{p}_1=(3.5,0,0)\text{Å}$, $\mathbf{p}_2=(3.3,1.2,-0.7)\text{Å}$.
2. Case 2 $(n=6,m=6)$. $\theta_2=\pi/6,\theta_1=\pi/6$. $\mathbf{t}_2=(0,0,1.23)\text{Å}$, $\mathbf{t}_1=(0,0,-1.23)\text{Å}$, $\mathbf{p}_1=(4.1,0,0)\text{Å}$, $\mathbf{p}_2=(3.82,1.39,0)\text{Å}$.

4.3. Specification of the subgroup and fundamental domain

In this section we define the subgroup G and a fundamental domain $\mathscr{D}$, or, for a carbon nanotube. By definition, a fundamental domain $\mathscr{D}\subset\mathbb{R}^3$ of G is a region with the properties that (1) the group applied to $\mathscr{D}$ fills all of space and, (2) the images of $\mathscr{D}$ under the group are nonoverlapping: $(\mathbf{Q}_1\mathscr{D}+\mathbf{c}_1)\cap(\mathbf{Q}_2\mathscr{D}+\mathbf{c}_2)=\emptyset$ for distinct group elements $(\mathbf{Q}_1|\mathbf{c}_1)$, $(\mathbf{Q}_2|\mathbf{c}_2)$. Within the fundamental domain we need to specify a number of position vectors, representing simulated atoms, and their initial positions and velocities. In practice it would only be necessary to specify this domain in a suitable neighborhood of a cylinder that coincides with the (say $T=0$) nanotube.

In reality, to put into practice the method, knowledge of the fundamental domain is unnecessary. That is, one can place any number of atoms at any positions, map these to other locations using the subgroup, simulate the equations of molecular dynamics using just the original set of atoms while calculating the forces on these from all other atoms, and, finally, ensure at every time step that the other atoms continue to be given as the group orbit of the original set. However, for most applications, one wants to simulate the motions of atoms that are reasonably close to a given structure which is, say, an objective molecular structure. In that case one wants to consider a fundamental domain (and subgroup) corresponding to that structure. Then one chooses the number of atoms in the fundamental domain, and their initial positions, to be reasonably close to those for given structure.

Thus, the subgroup, fundamental domain and simulated atoms have to be chosen rather carefully, so as to be compatible with the equilibrium structures of Cases 1 and 2. First we notice that for these structures there are an infinite number of pairs (p,q) that give each atom. This is related to the observation that the formula (51) is constructed from the two helices of points $\sum_{i=0}^{p-1}\mathbf{R}_2^i\mathbf{t}_2$ and $\sum_{i=0}^{q-1}\mathbf{R}_1^i\mathbf{t}_1$ and these intersect each other at an infinite number of points.

To begin the construction of useful subgroups and we begin at $(p,q)=(0,0)$ and we follow each of the helices to the first intersection point. That is, we find the integers $(\bar{p},\bar{q})$, smallest in absolute value, that satisfy

$$\sum_{i=0}^{\bar{p}-1}\mathbf{R}_2^i\mathbf{t}_2=\sum_{i=0}^{\bar{q}-1}\mathbf{R}_1^i\mathbf{t}_1. \tag{63}$$

Straightforward calculations show that (63) is equivalent to the two conditions:

$$\mathbf{R}_2^{\bar{p}}=\mathbf{R}_1^{\bar{q}}\quad\text{and}\quad\bar{p}(\mathbf{t}_2\cdot\mathbf{e}_3)=\bar{q}(\mathbf{t}_1\cdot\mathbf{e}_3), \tag{64}$$

where $\mathbf{e}_3$ is a unit vector on the common axis of $\mathbf{R}_1$ and $\mathbf{R}_2$, as above. This gives the following:

1. Case 1. $\bar{p}=9$ and $\bar{q}=0$.
2. Case 2. $\bar{p}=6$ and $\bar{q}=-6$.

This gives us a way to remove the degeneracy of multiple labels for points, by restricting the indices (p,q). That is, restricting to the strip confined by consecutive turns of one of the helices ensures that we obtain a unique labeling of points on the nanotube. That is, we restrict $(p,q)\in\mathbb{Z}^2$ to the following in each case:

1. Case 1. $0\leqslant p<9$ and $-\infty<q<\infty$.
2. Case 2. $0\leqslant p<6$ and $-\infty<q<\infty$.

We note that this choice is not unique. One can take the points labeled by $(0,0)$ and any choice of (p,q) and this generates a helix through these two points. Then the region between consecutive turns of the helix defines a suitable strip that gives unique labels of all points on the nanotube.

The definition of $(\bar{p},\bar{q})$ given above, either (63) or (64), implies that $\mathbf{x}_{(\bar{p},0),k}=\mathbf{x}_{(0,\bar{q}),k}$. But it actually implies much more.

Lemma 4.1. *If* $\mathbf{R}_2^{\bar{p}}=\mathbf{R}_1^{\bar{q}}$ *and* $\bar{p}(\mathbf{t}_2\cdot\mathbf{e}_3)=\bar{q}(\mathbf{t}_1\cdot\mathbf{e}_3)$, *then*

$$\mathbf{x}_{(p,q),k}=\mathbf{x}_{(p+\bar{p},q-\bar{q}),k} \tag{65}$$

for all integers (p,q) *and* $k=1,\ldots,M$.

Proof. We have to check whether, under the given hypotheses,

$$\sum_{i=0}^{p+\bar{p}-1}\mathbf{R}_2^i\mathbf{t}_2+\mathbf{R}_2^{p+\bar{p}}\sum_{i=0}^{q-\bar{q}-1}\mathbf{R}_1^i\mathbf{t}_1+\mathbf{R}_2^{p+\bar{p}}\mathbf{R}_1^{q-\bar{q}}\mathbf{p}_k=\sum_{i=0}^{p-1}\mathbf{R}_2^i\mathbf{t}_2+\mathbf{R}_2^p\sum_{i=0}^{q-1}\mathbf{R}_1^i\mathbf{t}_1+\mathbf{R}_2^p\mathbf{R}_1^q\mathbf{p}_k, \tag{66}$$

that is, after cancelling the terms involving $\mathbf{p}_k$, whether

$$\sum_{i=p}^{p+\bar{p}-1}\mathbf{R}_2^i\mathbf{t}_2+\mathbf{R}_2^{p+\bar{p}}\sum_{i=0}^{q-\bar{q}-1}\mathbf{R}_1^i\mathbf{t}_1-\mathbf{R}_2^p\sum_{i=0}^{q-1}\mathbf{R}_1^i\mathbf{t}_1=0. \tag{67}$$

This is in turn equivalent to

$$\sum_{i=0}^{\bar{p}-1}\mathbf{R}_2^{p+i}\mathbf{t}_2+\mathbf{R}_2^{p+\bar{p}}\sum_{i=0}^{q-\bar{q}-1}\mathbf{R}_1^{i}\mathbf{t}_1-\mathbf{R}_2^{p}\sum_{i=0}^{q-1}\mathbf{R}_1^{i}\mathbf{t}_1$$
$$=\mathbf{R}_2^{p}\left[\sum_{i=0}^{\bar{p}-1}\mathbf{R}_2^{i}\mathbf{t}_2+\mathbf{R}_2^{\bar{p}}\sum_{i=0}^{q-\bar{q}-1}\mathbf{R}_1^{i}\mathbf{t}_1-\sum_{i=0}^{q-1}\mathbf{R}_1^{i}\mathbf{t}_1\right]=0. \tag{68}$$

Now examine the middle term in the brackets:

$$\mathbf{R}_2^{\bar{p}}\sum_{i=0}^{q-\bar{q}-1}\mathbf{R}_1^{i}\mathbf{t}_1=\mathbf{R}_1^{\bar{q}}\sum_{i=0}^{q-\bar{q}-1}\mathbf{R}_1^{i}\mathbf{t}_1=\sum_{i=\bar{q}}^{q-1}\mathbf{R}_1^{i}\mathbf{t}_1=\sum_{i=0}^{q-1}\mathbf{R}_1^{i}\mathbf{t}_1-\sum_{i=0}^{\bar{q}-1}\mathbf{R}_1^{i}\mathbf{t}_1. \tag{69}$$

Replacing the middle term back in (68), we see that this expression does indeed vanish (cf. (63)), proving the lemma. □

Now return to the basic invariance condition

$$\mathbf{x}_{v+\eta,k}=\mathbf{Q}_\eta\mathbf{x}_{v,k}+\mathbf{c}_\eta,\quad \eta^j=\mu_i^j\zeta^i. \tag{70}$$

This invariance condition is consistent with the condition $\mathbf{x}_{(p,q),k}=\mathbf{x}_{(p+\bar{p},q-\bar{q}),k}$ in the following sense. That is, if we put $\eta=(\bar{p},-\bar{q})$ in (70), and notice that

$$\mathbf{Q}_\eta=\mathbf{Q}_{(\bar{p},-\bar{q})}=\mathbf{R}_2^{\bar{p}}\mathbf{R}_1^{-\bar{q}}=\mathbf{I}, \tag{71}$$

and also that

$$\begin{aligned}\mathbf{c}_\eta=\mathbf{c}_{(\bar{p},-\bar{q})}&=\sum_{i=0}^{\bar{p}-1}\mathbf{R}_2^{i}\mathbf{t}_2+\mathbf{R}_2^{\bar{p}}\sum_{i=0}^{\bar{q}-1}\mathbf{R}_1^{i}\mathbf{t}_1\\&=\sum_{i=0}^{\bar{p}-1}\mathbf{R}_2^{i}\mathbf{t}_2+\mathbf{R}_1^{\bar{q}}\sum_{i=0}^{\bar{q}-1}\mathbf{R}_1^{i}\mathbf{t}_1\\&=\sum_{i=0}^{\bar{p}-1}\mathbf{R}_2^{i}\mathbf{t}_2-\sum_{i=0}^{\bar{q}-1}\mathbf{R}_1^{i}\mathbf{t}_1\\&=0.\end{aligned} \tag{72}$$

Therefore the key point for assuring that the $(T=0)$ structure of the carbon nanotube is preserved by the choice of subgroup and fundamental domain is that $\eta=(\bar{p},-\bar{q})$ is achieved by some pair of integers $\zeta=(\zeta^1,\zeta^2)$. That is, for some such pair, we have that

$$\mu_i^j\zeta^i=\eta^j\quad\text{where }(\eta^1,\eta^2)=(\bar{p},-\bar{q}). \tag{73}$$

Equivalently, we have that

$$\mu^{-1}\begin{pmatrix}\bar{p}\\-\bar{q}\end{pmatrix}\in\mathbb{Z}^2. \tag{74}$$

We simply choose an invertible matrix of integers μ_i^j consistent with (74). We use this to define the subgroup. As explained above the simulated atoms consist of the pairs of integers in the parallelogram confined by the two vectors (μ_1^1,μ_1^2) and (μ_2^1,μ_2^2); more

precisely, the pairs of integers in the region

$$\{\lambda_1(\mu_1^1,\mu_1^2)+\lambda_2(\mu_2^1,\mu_2^2):\sum\lambda_i\leqslant 1,0\leqslant\lambda_i<1\}. \tag{75}$$

We call this set the *objective domain*. It gives a convenient representation of atoms whose positions are in the fundamental domain.

In the next section we will choose various subgroups by making various choices of μ_i^j. It will be useful to notice a quick way to get these subgroups corresponding for arbitrary (n,m)-nanotube. It is easily seen that these subgroups are obtained using the same basic formulas (51)–(62) as for the full nanotube, but substituting (μ_1^1,μ_1^2) for $(1,0)$ and (μ_2^1,μ_2^2) for $(0,1)$ in (57) and (62). We will use capital letters $(\Theta_1,\Theta_2,\mathbf{T}_1,\mathbf{T}_2)$ (in place of $(\theta_1,\theta_2,\mathbf{t}_1,\mathbf{t}_2)$) to denote these kinematic quantities for these subgroups. They are given by:

$$\Theta_2=2\pi\xi(\mu_1^1,\mu_1^2)\quad\text{and}\quad\Theta_1=2\pi\xi(\mu_2^1,\mu_2^2), \tag{76}$$

$$\mathbf{T}_2=\eta(\mu_1^1,\mu_1^2)\mathbf{e}_3\quad\text{and}\quad\mathbf{T}_1=\eta(\mu_2^1,\mu_2^2)\mathbf{e}_3. \tag{77}$$

We also use the notation (c.f., (53))

$$\mathscr{R}_1=\mathbf{Q}_{\Theta_1}\quad\text{and}\quad\mathscr{R}_2=\mathbf{Q}_{\Theta_2}. \tag{78}$$

4.4. Classical objective molecular dynamics simulations of carbon nanotubes

4.4.1. From translational to objective molecular dynamics

For the purpose of testing the above ideas we have implemented the objective MD scheme in the context of classical molecular dynamics. From the multitude of the available potentials to model the carbon–carbon covalent bonding we have selected the three body potential given by Tersoff (1988), already implemented into a periodic MD scheme in the computational package Trocadero (Rurali and Hernandez, 2003). The employed carbon parameters were taken from Saada et al. (1999). Our aim is not to give a detailed quantitative study of carbon nanotubes, but rather to illustrate the capabilities of the method.

As explained at the end of the preceding section, we will use the set of quantities $\Theta_2,\Theta_1,\mathbf{T}_2,\mathbf{T}_1$ to define the subgroup. The simulated atomic positions will be denoted by $\mathbf{P}_1,\ldots,\mathbf{P}_M$, $M=2|\det\mu|$. That is, following the remark after (75), the two-term formula with $\Theta_2,\Theta_1,\mathbf{T}_2,\mathbf{T}_1$ and "molecule" $\mathbf{P}_1,\ldots,\mathbf{P}_M$ expresses how atoms are related in the objective MD scheme, and this formula, with appropriate choice of $\mathbf{P}_1,\ldots,\mathbf{P}_M$ is compatible with the usual assignment of $(T=0)$ atomic positions for the full nanotube. In short, the scheme is defined by the formula

$$\mathbf{X}_{(\zeta^1,\zeta^2),k}=\mathbf{X}_1+\sum_{i=0}^{\zeta^1-1}\mathscr{R}_2^i\mathbf{T}_2+\mathscr{R}_2^{\zeta^2}\sum_{i=0}^{\zeta^2-1}\mathscr{R}_1^i\mathbf{T}_1+\mathscr{R}_2^{\zeta^1}\mathscr{R}_1^{\zeta^2}\mathbf{P}_k. \tag{79}$$

The set of parameters $\Theta_2,\Theta_1,\mathbf{T}_2,\mathbf{T}_1$ represents input data for the computational scheme. With given initial conditions, the simulated atoms have time-dependent positions $\mathbf{P}_1(t),\ldots,\mathbf{P}_M(t),t>0$ and the full set of atoms have time-dependent positions $\mathbf{X}_{(\zeta^1,\zeta^2),k}(t)$ given by (79).

To adapt the existing periodic MD format of Trocadero to the objective case, there are two issues that need to be addressed, namely (i) the replacement of periodicity conditions with the objective relations between replicas and (ii) the handling of symmetry arising out

of Newton's third law for the computed pair forces. Concerning issue (i), we use (79) together with a neighbor search to find atoms within the cutoff of the atomic forces. The neighbor search routine calculates the distance between the atom with position $\mathbf{P}_i(t) = \mathbf{X}_{(0,0),i}(t)$ in the fundamental domain and atom k from the (ζ^1, ζ^2) replica, situated at $\mathbf{X}_{(\zeta^1,\zeta^2),k}(t)$. If within the model's cutoff radius, atom k is validated as a neighbor of i, a force contribution on i due to neighbor k, $\mathbf{F}_{ik}$, is then computed. Regarding the second issue (ii), the pair force assigned to the atom $\mathbf{X}_{(\zeta^1,\zeta^2),k}(t)$, equals $-\mathbf{F}_{ik}$ by Newton's third law. This contribution is "passed" to the atom k situated in the fundamental domain through the objectivity transformation

$$\mathbf{F}_{ki} = -\mathscr{R}_2^{-\zeta^1}\mathscr{R}_1^{-\zeta^2}\mathbf{F}_{ik}. \tag{80}$$

Note that the periodic case is regained if both $\mathscr{R}_2$ and $\mathscr{R}_1$ are identity matrices.

With these two conceptual modifications we were able to successfully perform classical objective MD simulations on carbon nanotubes. We provide next a general description of how to manipulate the parameters of an objective MD simulation, so as to prescribe an axial strain and twist, and then discuss as an example application the torsional instabilities of carbon nanotubes.

4.4.2. *Objective molecular dynamics simulations*

An interesting observation related the discussion at the end of Section 4.3 is that an objective domain for one nanotube can serve as the objective domain for nanotubes of other chirality and radius if the input parameters $\Theta_2, \Theta_1, \mathbf{T}_2, \mathbf{T}_1$ are adjusted according to Eqs. (76) and (77). Thus, a large class of nanotubes can be efficiently simulated only by modifying these input parameters. This is not the case with the traditional periodic MD (based on axial periodicity), which requires a rather high minimum number of atoms depending on the nanotube radius and chiral angle. For this reason calculations on chiral tubes (with $\chi \neq 0$ or 30°) are rare. Both observations point to the flexibility of objective MD.

To select an objective domain we made the particular choice $\mu_1 = (3,0)$ and $\mu_2 = (0,3)$ corresponding to the shaded area of Fig. 3. The condition (74) holds for both $(9,0)$ and $(6,6)$ nanotubes and in general for all nanotubes whose n and m indices are multiples of 3. The resulting parameters are $\Theta_2 = 2\pi\xi(3,0) = 3\theta_2, \Theta_1 = 2\pi\xi(0,3) = 3\theta_1$, $\mathbf{T}_2 = \eta(3,0)\mathbf{e}_3, \mathbf{T}_1 = -\eta(0,3)\mathbf{e}_3$ and there are $M = 2|\det\mu| = 18$ simulated atoms.

Having decided on the objective domain, we can now start an MD run. As indicated above, objective MD allows certain large-scale dynamic modes. To illustrate this point we started a cold simulation (velocities were taken to be zero) on a 18-atom patch with the $\Theta_2, \Theta_1, \mathbf{T}_2, \mathbf{T}_1$ adjusted for a (12,12) tube. Purposely, the atomic positions (given by formula (49)) were assigned a 7% larger radius. This way all initial phonons will be contained in the out-of-plane A_1 vibrational mode, which couples to the radial breathing motion of a tube. The 18-atom objective domain was evolved with a velocity Verlet algorithm with a time step of 1 fs. In order to monitor the occupancy of the breathing mode, we can simply plot the time evolution of the average CNT radius. The results of Fig. 4(a) suggest an apparent initial damping of the breathing vibrations, followed by almost a full revival, after 40 ps. Thus, under the radial expansion initial conditions, the lattice motion is contained in the large-scale breathing oscillations. In simulations corresponding to Fig. 4(b), the atoms were given an additional 7% displacement along the

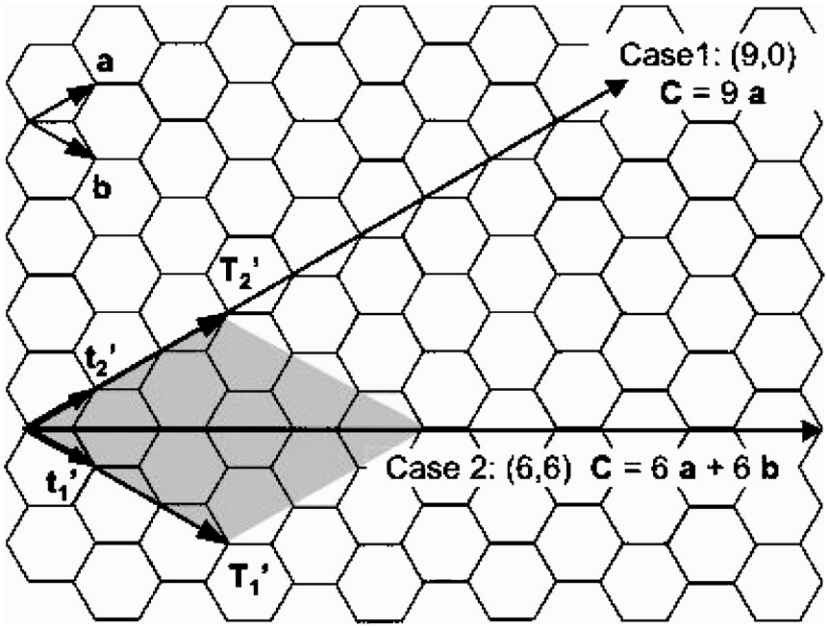

Fig. 3. Objective domain (shaded area) for both the (6, 6) and (9, 0) nanotubes. $\mathbf{T}_1'$ and $\mathbf{T}_2'$ indicate, in the unrolled representation, the vectors $\mathbf{T}_1$ and $\mathbf{T}_2$ vectors given by relation (77) and used in the objective description (79). Indices corresponding to the 18 simulated atoms lie the objective domain.

nanotube axis. The time evolution of the average radius suggests that the addition of this higher energy axial mode facilitates the passage of energy from the large-scale breathing mode into small-scale atomic level vibrations, in the spirit of studies of Fermi et al. (1955). For comparison, Fig. 4(c) displays the same quantity measured from a periodic MD simulation with an 384-atom translational supercell, which initially was given the 7% radial increase. Thermalization is now achieved on a few ps time scale. Fig. 4(d) plots the time evolution of temperatures for the simulations shown in (a) and (c), and supports the same conclusions: while in the periodic MD case a thermal equilibrium is established around the 400 K, the large temperature oscillations around the same average value suggest that equilibration was not reached in the objective MD case.

It is important to notice that, while the angles Θ_2, Θ_1 given by formula (76) depend only on the choice of μ, the $\mathbf{T}_2$ and $\mathbf{T}_1$ vectors given by (77) depend also on the parameter l_{C-C}, the bond length on the sheet before rolling. To relieve a possible strain along the nanotube axis and obtain the relaxed values of $\mathbf{T}_2$ and $\mathbf{T}_1$ belonging to a specific (n, m) tube, we have performed potential energy surface scans as a function of l_{C-C} (viewed now as a parameter) under the constraints of fixed Θ_2 and Θ_1 and fixed fraction $|\mathbf{T}_1|/|\mathbf{T}_2| = -\eta(0,3)/\eta(3,0) = n/m$. Relaxations were performed with a conjugate gradient scheme. The relaxation tolerance was of 10^{-6} a.u. for energy and 10^{-4} a.u. for the atomic forces.

For each value of l_{C-C} the relaxed nanotube adopts a particular radius R. It is useful to plot the calculated energies (measured per atom and relative to a flat patch) of the relaxed 18-atom patches belonging to various (n, m) tubes as function of $1/R^2$ (Fig. 5). As expected in view of the isotropic properties of a graphite layer in the linear regime, the bending

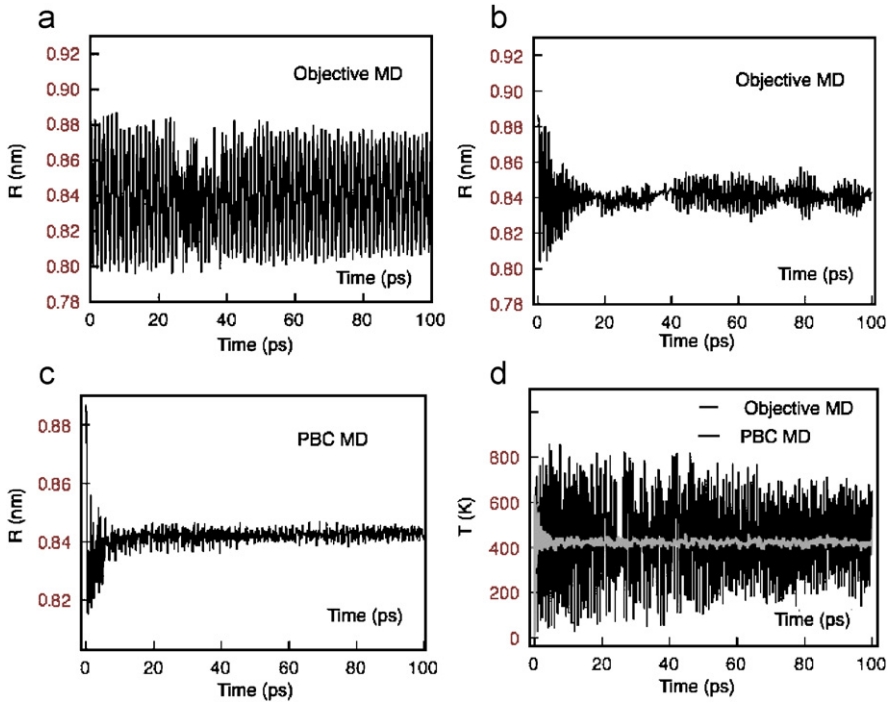

Fig. 4. MD simulation of a (12,12) carbon nanotube to study the passage of energy from large-scale to small-scale modes: From an 18-atom objective MD simulations, (a) and (b) shows the evolution of the average radius when simulation starts from distinct initial conditions. Time evolution of the (c) tube radius in a PBC MD and of the (d) temperature in both MD types.

energy E_b shows no chirality dependence. We have found that the dependence on curvature can be described with great precision by the formula $E = 1/2DR^{-2}$, where the constant $D = 29.2\,\text{meV}\,\text{nm}^2/\text{atom}$ represents the flexural rigidity of the graphite layer.

From the above discussion it is now obvious that, having the equilibrium values for $\mathbf{T}_2$ and $\mathbf{T}_1$ at zero temperature, imposing a longitudinal strain ε on the patch can be done by changing $\mathbf{T}_1$ and $\mathbf{T}_2$ to $(1+\varepsilon)\mathbf{T}_1$ and $(1+\varepsilon)\mathbf{T}_2$ (which does not change $|\mathbf{T}_1|/|\mathbf{T}_2| = n/m$) and keeping the angles Θ_2 and Θ_1 fixed. The average radius of the nanotube will relax during the simulation, allowing for a Poisson contraction.

The procedure for applying an arbitrary axial twist per unit length of $\alpha\,\text{rad}/\text{nm}$ at fixed strain is as follows: while preserving the equilibrium values for $\mathbf{T}_2$ and $\mathbf{T}_1$, the angles Θ_2 and Θ_1 are modified to $\Theta_2 + \alpha|\mathbf{T}_2|$ and $\Theta_1 - \alpha|\mathbf{T}_1|$. This simple procedure contrasts with the relative rigidity imposed by periodic MD, where α is constrained by the rotational symmetry of the tube and the number of unit cells.

We performed structural relaxations on twisted nanotubes with the same 18-atom objective domain. We found a linear regime where the energy per length varied as $E_l = 1/2K\alpha^2$, and we interpreted K as the torsional modulus. For a twisted hollow thin walled cylinder in the linear elastic regime, it is expected that K will have a linear dependence with the cube of the tube radius, which was obtained from the simulation in each case. The results displayed in Fig. 6 confirm this expectation. Moreover, the tube

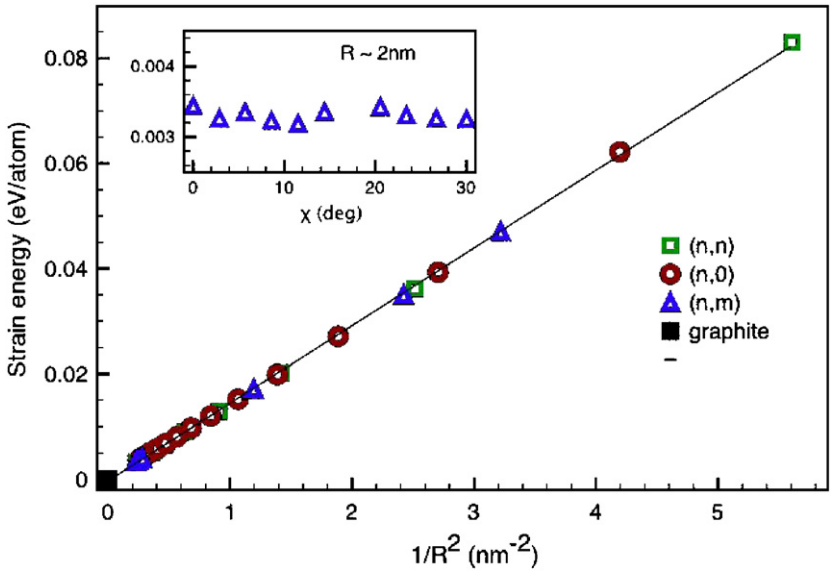

Fig. 5. Curvature-strain energy for nanotubes as a function of the square of their inverse radius. The insert shows the dependence with chirality (χ) for an approximately equal-radius family of tubes. Data were obtained using an objective domain containing 18 atoms corresponding to the shaded area of Fig. 3. The n and m indices are multiples of 3.

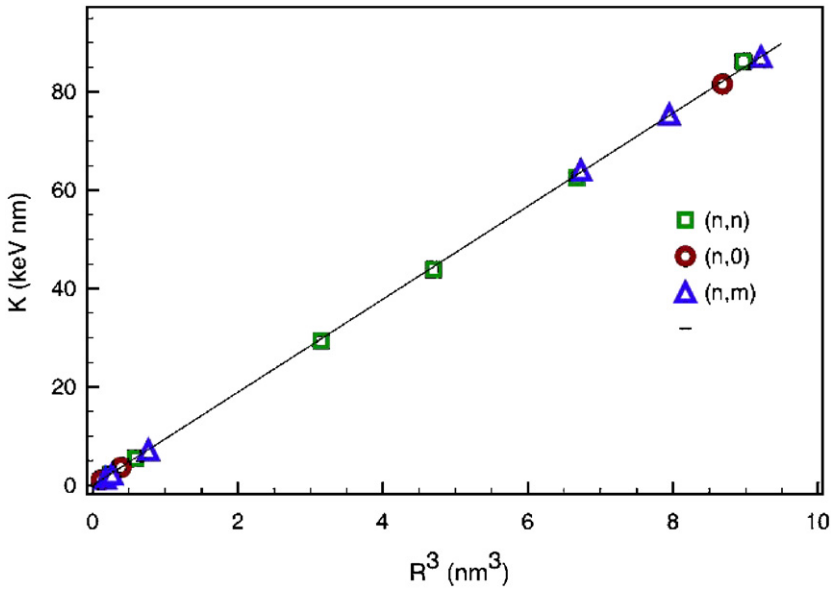

Fig. 6. Torsional modulus K versus the cube of the nanotube radius. The 18-atom objective domain shown in Fig. 3 was used in all simulations and armchair ($n = 9, 12, 21, 24, 27, 30$), zigzag ($n = 12, 18, 51$), and chiral [(12, 3), (12, 6), (21, 3), (30, 24), (33, 24), (33, 27), (45, 12), (48, 6)] tubes were simulated.

chirality does not show any influence on the graph. A more precise fitting yields $K = (9232 \pm 114) \cdot (R/nm)^{3.033 \pm 0.019}$ eV nm. The calculation for K was performed for a small α range, from 0° to 2°/nm, in which no deviations from the quadratic dependence of the strain energy on α were observed.

Next, we indicate the utility of objective MD method in situations involving bifurcation and complex shape changes. The examples presented in Fig. 7 demonstrate that the objective MD can describe severe buckling patterns that arise when a (12,12) tube is subjected to a twist of $\alpha = 10^\circ$/nm.

The structure with four azimuthal lobes shown in Fig. 7(a) was obtained using both periodic MD (axial periodicity) with a fundamental domain containing 1728 atoms and objective MD using the objective domain shown in Fig. 7(b). This domain follows the circumference (in the $\mathbf{T_1}$ direction) and the helical buckling (along $\mathbf{T_2}$). It is characterized by $\mu_1 = (5, -3)$ and $\mu_2 = (3, 3)$, the angles $\Theta_2 = \pi/6$ and $\Theta_1 = \pi/2$, and contains 48 atoms.

As suggested by the continuum treatment for buckling of cylindrical shell subjected to torsion (Timoshenko, 1936), the nonlinear response of a carbon nanotube is expected to involve skew harmonic modes with a distinct number of azimuthal lobes and half waves along the tube axis. While the study of various modes is cumbersome when using periodic MD, it can be readily done on carefully selected domains compatible with the skew harmonics. Starting with the domain represented in Fig. 7(b), two larger domains with rotation angles Θ_1 of $2\pi/3$ and π can be obtained by changing μ_2 to (4,4) and (6,6), respectively. Objective relaxation of the perfect cylindrical nanotube built from these new domains leads to the lower energy modes having three and two azimuthal lobes and the same axial period. The configurations we obtained (after further relaxations) are displayed in Figs. 7(c) and (d). Note that objective MD study of modes with different axial periods is also possible and this would require similar adjustments in the $\mathbf{T_2}$ direction.

The objective MD capability of allowing an arbitrary twist along with the ability to study in a decoupled way the distinct deformation modes allows one to precisely pinpoint the critical level of twist beyond which the cylinder shape becomes unstable, i.e., the bifurcation point. The results of a series of careful energy minimizations are summarized in Fig. 8, where plots of energy vs. the twist angle α are shown for three choices of objective domains. In each case the axial stress was relaxed in the same manner as described above. The upper dotted curve uses a two-atom objective domain with $\theta_2 = \pi/12$. Clearly, none of the deformation modes of Fig. 7 can be described using this domain, which preserves the perfect cylindrical shape. The two lowest curves correspond to objective domains used for the two ($\Theta_1 = \pi$) and three ($\Theta_1 = 2\pi/3$) lobe modes of Figs. 7(d) and (c), respectively. At a critical level of about 2°/nm twist the perfect structure can lower its energy by assuming the two-lobe state or the three-lobe state at slightly higher α; the two bifurcations are very close together as indicated. Another interesting feature is that these transitions occur with significant length changes. The inset of Fig. 8 summarizes the obtained twist-induced length changes for the three investigated modes. Interestingly, while the perfect structure has the tendency to elongate under α, the spirally buckled morphologies are significantly shorter than the no twist state. This means that if axial relaxation is prevented a considerable amount of axial stress can be stored in the tubule. We emphasize that although the nonlinear instabilities under torsion have been noticed before (Yakobson et al., 1996; Zhang et al., 2005), the objective approach allows for an unprecedented characterization of bifurcation points and a decoupled study of the various response modes.

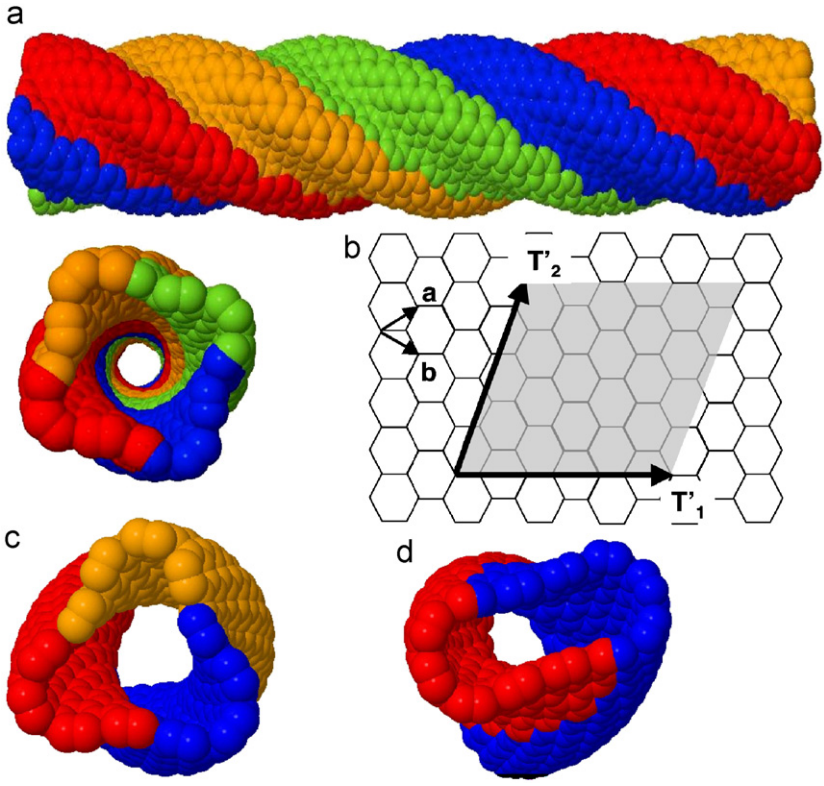

Fig. 7. Response of a (12,12) nanotube exposed to a $10^\circ/\text{nm}$ twist. (a) The structure with four azimuthal lobes (shown in the axial and transversal view), was obtained using both a translational unit cell (upper) and the objective domain shown in (b). The vector $\mathbf{T}_1'$ is along the tube circumference and $\Theta_1 = \pi/2$. Three (c) and two (d) azimuthal lobes were obtained when the domain was expanded along $\mathbf{T}_1$ and Θ_1 was correspondingly changed to $\Theta_1 = 2\pi/3, \pi$. All structures shown were reconstructed from the objective domain shown by using the relation (79). Colors correspond to distinct azimuthal replicas of the objective domain.

In general, one must expect that in an objective molecular dynamics simulation the overall features of the results, e.g., the number of lobes in the example above, can depend on the choice of the fundamental domain. Thus, while the simulation represents exact molecular dynamics in the limit of vanishing time step, it may not represent "typical" molecular dynamics. That is, the solution obtained from generic initial conditions may have different overall features. The situation is familiar from periodic molecular dynamics, where a doubling of the size of the supercell can sometimes give different results. In practical terms a firm prediction is better supported by several simulations using several fundamental domains, especially in cases that the wavelength of an instability is of the order of the size of the fundamental domain.

Finally, we indicate how objective method can be used to study bending deformations in nanotubes: in the framework provided by formula (79), bending can be imposed via the rotation matrix $\mathscr{R}_1$ and by choosing $\mathscr{R}_2 = \mathbf{I}$, $\mathbf{T_1} = \mathbf{T_1} = 0$, while the selected simulation domain should capture the full circumference of the tube. Effectively, these choices reduce the two-term formula to the one-term formula. Fig. 9 shows results from a series of

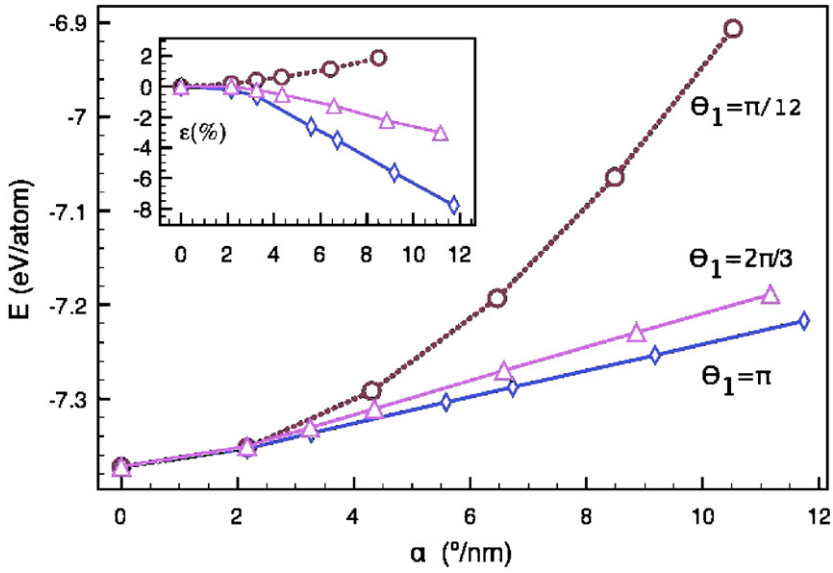

Fig. 8. Energy of a (12,12) nanotube as a function of the twist angle α. The lowest modes of Fig. 7(d) and Fig. 7(c) emerge at about 2°/nm. Upper curve corresponds to the perfect cylindrical shape. The marked Θ_1 values correspond to the used objective domains. Inset shows the axial strain induced by twisting.

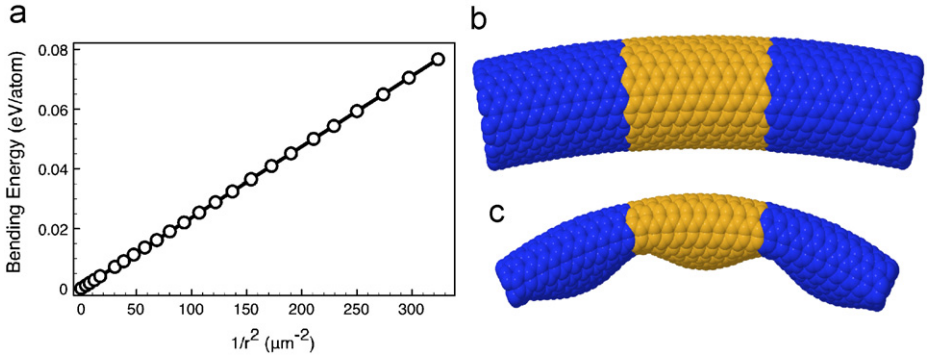

Fig. 9. (a) Energy of a (12,12) nanotube as a function of the square of bending curvature. Nanotube structure in the (b) linear ($\Theta_1 = 6^\circ$, $r = 21$ nm) and (c) nonlinear ($\Theta_1 = 20^\circ$, $r = 7.1$ nm) bending regime. Simulations employ a 480-atom periodic cell shown in yellow (light gray).

optimization calculations performed on a translational cell containing 480 atoms from a (12,12) tube. At small bending (Figs. 9a and b) the energy measured per atom grows as $E_B = (1/2)kr^{-2}$, where $k = 6.23\,\text{meV}\,\mu\text{m}^2$. The optimized bent geometry of Fig. 9b shows the simulation domain (yellow) and two replicas (blue) obtained with formula (79). Under higher bending, for $\Theta_1 = 20^\circ$, the emergence of buckling can be observed in Fig. 9c.

Overall, we have illustrated in this section how the objective MD method based on a classical potential (Tersoff) can be useful in studying the mechanical response of carbon nanotubes. Due to the typically small number of atoms contained in an objective domain,

it is computationally attractive to use the proposed scheme in conjunction with more precise tight-binding (Hua et al., in preparation) or first principles potentials. We note, as discussed in James (2006), both tight-binding and density functional theory methods for computing the energy of a particular configuration can also be simplified by using objective boundary conditions.

Acknowledgment

This work was carried out at the Minnesota Supercomputing Institute. TD acknowledges support from MRSEC-NSF DMR-0212302, and NSF-NIRT CTS-0506748. The work of RDJ was supported by DOE, DE-FG02-05ER25706, NSF-NIRT, DMS-0304326, AFOSR STTR, FA9550-05-C-0035, and the AH-PCRC. He is also pleased to acknowledge the support of the Humboldt Foundation, and the hospitality of the MPI-MIS.

References

Allen, M.P., Tildesley, D.J., 1987. Computer Simulation of Liquids. Oxford University Press, Oxford.

Caspar, D.L.D., Klug, A., 1962. Physical principles in the construction of regular viruses. Cold Spring Harbor Symp. Quant. Biol. 27, 1–24.

Costanzo, F., Gray, G.L., Andia, P.C., 2005. On the definitions of effective stress and deformation gradient for use in MD: Hill's macro-homogeneity and the virial theorem. Int. J. Eng. Sci. 43, 533–555.

Crane, H.R., 1950. Principles and problems of biological growth. Sci. Mon. 70, 376–389.

Dumitrică, T., Hua, M., Yakobson, B.I., 2006. Symmetry, time, and temperature dependent strength of carbon nanotubes. Proc. Natl. Acad. Sci. USA 103, 6105–6109.

Falk, W., James, R.D., 2006. An elasticity theory for self-assembled protein lattices with application to the martensitic phase transition in bacteriophage T4 tail sheath. Phys. Rev. E 73, 011917.

Fermi, E., Pasta, J., Ulam, S., 1955. Studies of the nonlinear problems. Los Alamos Report LA-1940.

Freddolino, P.L., Arkhipov, A.S., Larson, S.B., McPherson, A., Schulten, K., 2006. Molecular dynamics simulations of the complete satellite tobacco mosaic virus. Structure 14, 437–449.

Hardy, R.J., 1982. Formulas for determining local properties in molecular dynamics simulations: shock waves. J. Chem. Phys. 76, 622–628.

Hua, M., Dumitrică, T., James, R.D., Tight Binding Objective Molecular Dynamics in preparation.

James, R.D., 2006. Objective structures. J. Mech. Phys. Solids 54, 2354–2390.

Murdoch, A.I., Bedeaux, D., 1994. Continuum equations of balance via weighted averages of microscopic quantities. Proc. R. Soc. London A 445, 157–179.

Parrinello, M., Rahman, A., 1980. Crystal structure and pair potentials: a molecular dynamics study. Phys. Rev. Lett. 45 (14), 1196–1199.

Popov, V., 2004. Curvature effects on the structural, electronic and optical properties of isolated single-walled carbon nanotubes within a symmetry-adapted non-orthogonal tight-binding model. New J. Phys. 6, 17.

Rurali, R., Hernandez, E., 2003. Trocadero: a multiple-algorithm multiple-model atomistic simulation program. Comput. Mater. Sci. 28, 85–106.

Saada, D., Adler, J., Kalish, R., 1999. Computer simulation of damage in diamond due to ion impact and its annealing. Phys. Rev. B 59, 6650–6660.

Tersoff, J., 1988. New empirical approach for the structure and energy of covalent systems. Phys. Rev. B 37, 6991–7000.

Timoshenko, S., 1936. Theory of Elastic Stability. McGraw-Hill, New York, p. 480.

Toukan, K., Carrion, F., Yip, S., 1983. Molecular dynamics study of structural instability of two-dimensional lattices. J. Appl. Phys. 56 (5), 1455–1461.

White, C.T., Robertson, D.H., Mintmire, J.W., 1993. Helical and rotational symmetries of nanoscale graphitic tubules. Phys. Rev. B 47, 5485–5488.

Yakobson, B.I., Brabec, C.J., Bernholc, J., 1996. Nanomechanics of carbon nanotubes: instabilities beyond linear response. Phys. Rev. Lett. 76, 2511–2514.

Zhang, S., Mielke, S.L., Khare, R., Troya, D., Ruoff, R.S., Schatz, G.C., Belytschko, T., 2005. Mechanics of defects in carbon nanotubes: Atomistic and multiscale simulations. Phys. Rev. B 71, 115403.

Zhou, M., 2005. Thermomechanical continuum representation of atomistic deformation at arbitrary size scales. Proc. R. Soc. London A 461, 3437–3472.

Zimmerman, J.A., Webb III, E.B., Hoyt, J.J., Jones, R.E., Klein, P.A., Bammann, D.J., 2004. Calculation of stress in atomistic simulation. Model. Simul. Mater. Sci. Eng. 12, S319–S332.